

Higher Structures

Nathalie Wahl; Oscar Harr; Max Vistrup
Disordered arcs and Harer stability

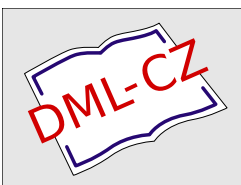
Higher Structures, Vol. 8 (2024), No. 1, 193–223

Persistent URL: <http://dml.cz/dmlcz/153468>

Terms of use:

© Institute of Mathematics, Czech Academy of Sciences, 2024

Institute of Mathematics of the Czech Academy of Sciences provides access to digitized documents strictly for personal use. Each copy of any part of this document must contain these *Terms of use*.



This document has been digitized, optimized for electronic delivery and stamped with digital signature within the project *DML-CZ: The Czech Digital Mathematics Library*
<http://dml.cz>

Disordered arcs and Harer stability

Oscar Harr^a, Max Vistруп^b and Nathalie Wahl^a

^aDepartment of Mathematical Sciences, University of Copenhagen, Universitetsparken 5, 2100 Copenhagen, Denmark

^bDep. Informatik, CNB H 106, Universitätstrasse 6, 8092 Zürich, Switzerland

Abstract

We give a new proof of homological stability with the best known isomorphism range for mapping class groups of surfaces with respect to genus. The proof uses the framework of Randal-Williams–Wahl and Krannich applied to disk stabilization in the category of bidecorated surfaces, using the Euler characteristic instead of the genus as a grading. The monoidal category of bidecorated surfaces does not admit a braiding, distinguishing it from previously known settings for homological stability. Nevertheless, we find that it admits a suitable Yang–Baxter element, which we show is sufficient structure for homological stability arguments.

Communicated by: Andrey Lazarev.

Received: 28th November, 2022. Accepted: 15th September, 2023.

MSC: 57R50; 57M07.

Keywords: Homological stability, mapping class groups.

1. Introduction

Let $S_{g,r}^s$ be an orientable surface of genus g with r boundary components and s punctures. The mapping class group $\Gamma(S_{g,r}^s) := \pi_0 \text{Homeo}(S_{g,r}^s \text{ rel } \partial S)$ of S satisfies *homological stability*: the homology group $H_i(\Gamma(S_{g,r}^s); \mathbb{Z})$ is independent of g and r when g is large relative to i . This stability result was originally proved by Harer in [14], and later improved by Ivanov, Boldsen and Randal-Williams [18, 6, 24], see also [15, 28, 16, 11]. We recast the result here as a stability theorem in the category of *bidecorated surfaces*, and give a new proof of the best known stability range using the most straightforward inductive argument originally designed by Quillen, and formalized in [25, 22]. Our proof at the same time illustrates how little is needed to run the stability machines of these two papers.

Email addresses: obh@math.ku.dk (Oscar Harr)
max.vistруп@inf.ethz.ch (Max Vistруп)
wahl@math.ku.dk (Nathalie Wahl)

© Oscar Harr, Max Vistруп and Nathalie Wahl, 2024, under a [Creative Commons Attribution 4.0 International License](https://creativecommons.org/licenses/by/4.0/).

DOI: [10.21136/HS.2024.04](https://doi.org/10.21136/HS.2024.04)

Our main stability result is the following, recovering precisely the ranges of [6, Thm 1] and [24, Thm 7.1 (i),(ii)]:

Theorem A. Let $S_{g,r}^s$ be as above, with $g, s \geq 0$ and $r \geq 1$. The map

$$H_i(\Gamma(S_{g,r}^s); \mathbb{Z}) \longrightarrow H_i(\Gamma(S_{g,r+1}^s); \mathbb{Z})$$

induced by gluing a pair of pants along one boundary component is always split injective, and an isomorphism when $i \leq \frac{2g}{3}$, and the map

$$H_i(\Gamma(S_{g,r+1}^s); \mathbb{Z}) \longrightarrow H_i(\Gamma(S_{g+1,r}^s); \mathbb{Z})$$

induced by gluing a pair of pants along two boundary components is an epimorphism when $i \leq \frac{2g+1}{3}$ and an isomorphism when $i \leq \frac{2g-2}{3}$.

Combining the two maps in the theorem gives a genus stabilization that is known to be close to optimal by a computation of Morita [23] and low dimensional computations, see Remarks 2.6 and 4.11. While we do not know whether the two ranges in the above statement can be individually improved, it is remarkable that three rather different proofs (those of Boldsen [6], Randal-Williams [24], and ours) end up with the exact same ranges.

A particular feature of our proof is that the two maps occurring in the theorem will be for us “the same map”, namely a disk stabilization in the category \mathcal{M}_2 of *bidecorated surfaces*. A bidecorated surface is a surface S with two marked intervals I_0, I_1 in its boundary. The two intervals may lie on the same or on different boundary components. Morphisms in \mathcal{M}_2 are mapping classes, i.e. isotopy classes of homeomorphisms, and \mathcal{M}_2 admits a monoidal structure $\#$ defined by identifying the marked intervals in pairs.

Our main example of a bidecorated surface will be the bidecorated disk D . As shown in Lemma 3.1, taking sums of the disk with itself in \mathcal{M}_2 produces surfaces of any genus: $D^{\#2g+1}$ is a surface $S_{g,1}$ of genus g with a single boundary component, while $D^{\#2g+2}$ is a surface $S_{g,2}$ of genus g with two boundary components, each containing a marked interval. To obtain any surface $S_{g,r}^s$ with $r \geq 1$, we will consider the object $S \# D^{\#2g}$ in \mathcal{M}_2 , for $S = S_{0,r}^s$ a genus 0 surface with r boundary components and s punctures. Now the maps in Theorem A are precisely the disk stabilization maps in \mathcal{M}_2 :

$$\text{Aut}_{\mathcal{M}_2}(S \# D^{\#2g}) \xrightarrow{\#D} \text{Aut}_{\mathcal{M}_2}(S \# D^{\#2g+1}) \xrightarrow{\#D} \text{Aut}_{\mathcal{M}_2}(S \# D^{\#2g+2})$$

for these particular choices of surfaces.

Theorem A is thus the statement that disk stabilization $\#D$ in \mathcal{M}_2 induces isomorphisms on the homology of these automorphism groups in a range. We show in the present paper that this result can be obtained as a direct application of the main result of [22], from which an additional stability statement with twisted coefficients automatically follows. We start by stating this additional result.

Twisted coefficients Fix $r \geq 1$ and $s \geq 0$. In our setting, a coefficient system F for the mapping class group $\Gamma(S_{g,r}^s)$ is a collection of $\mathbb{Z}[\Gamma(S_{g,r}^s)]$ -modules F_{2g} and $\mathbb{Z}[\Gamma(S_{g,r+1}^s)]$ -modules F_{2g+1} for each $g \geq 0$, together with maps

$$F_n \longrightarrow F_{n+1}$$

equivariant with respect to the disk stabilization and satisfying that a certain Dehn twist acts trivially on the image of F_n in F_{n+2} under double stabilization (see Definition 4.6). Given a coefficient system, one can define a notion of degree; a constant coefficient systems has degree 0 and for example the coefficient system $F_{2g+i} = H_1(S_{g,r+i}^s; \mathbb{Z})^{\otimes k}$, $i \in \{0, 1\}$, has degree k (see Example 4.7).

We obtain the following twisted stability result:

Theorem B. Let $\Gamma(S_{g,r}^s)$ be as in Theorem A, and F be a coefficient system of degree k . The stabilization map

$$H_i(\Gamma(S_{g,r}^s); F_{2g}) \longrightarrow H_i(\Gamma(S_{g,r+1}^s); F_{2g+1})$$

is an epimorphism for $i \leq \frac{2g-3k-2}{3}$ and an isomorphism for $i \leq \frac{2g-3k-5}{3}$, and the map

$$H_i(\Gamma(S_{g,r+1}^s); F_{2g+1}) \longrightarrow H_i(\Gamma(S_{g+1,r}^s); F_{2g+2})$$

is an epimorphism for $i \leq \frac{2g-3k-1}{3}$ and an isomorphism for $i \leq \frac{2g-3k-4}{3}$. In these bounds, $3k$ can be replaced by k if F is in addition split in the sense of Definition 4.6.

Stability theorems for mapping class groups with twisted coefficients can be found in the work of Ivanov, Boldsen, Randal-Williams–Wahl, and Galatius–Kupers–Randal-Williams [6, 19, 25, 11]. The results are not easy to compare as the types of coefficient system that are permitted depend on the paper, but some classical examples such as the one described above fit all frameworks (see Remarks 4.8 and 4.11 for more details).

Braided action and Yang–Baxter operators We want to obtain Theorems A and B as consequences of Theorems A and C of [22]. For this, we first have to show that disk stabilization in the monoidal category $(\mathcal{M}_2, \#)$ comes from an action of a braided monoidal groupoid.

Let \mathcal{B} denote the groupoid of braid groups, with object the natural numbers and the braid group B_n as automorphisms of n . We will construct an action of \mathcal{B} on \mathcal{M}_2 using an appropriate *Yang–Baxter operator* in \mathcal{M}_2 : The sum of bidecorated disks $D \# D$ in \mathcal{M}_2 is a cylinder, whose mapping class group is an infinite cyclic group generated by the Dehn twist T along the core circle of the cylinder. It turns out that this morphism $T \in \text{Aut}_{\mathcal{M}_2}(D \# D)$ is a Yang–Baxter operator in \mathcal{M}_2 , in the sense that it satisfies the equation

$$(T \# 1)(1 \# T)(T \# 1) = (1 \# T)(T \# 1)(1 \# T)$$

in $\text{Aut}_{\mathcal{M}_2}(D^{\#3})$. The same holds for the inverse twist T^{-1} , that will turn out more convenient for us. As explained in Section 5.1, we get an associated strong monoidal functor $\mathcal{B} \longrightarrow \mathcal{M}_2$ taking the object n to $D^{\#n}$. The corresponding homomorphism $B_n \longrightarrow \text{Aut}_{\mathcal{M}_2}(D^{\#n})$ can be identified with the geometric embedding in the sense of [29], associated to the chain of curves a_1, \dots, a_{n-1} in

$$D^{\#n} = D \# D \# \dots \# D,$$

where the i th curve a_i is the core circle in the i th cylinder $D \# D$ in the above sum, see Lemma 3.5 and Example 5.3.

The strong monoidal functor $\mathcal{B} \longrightarrow \mathcal{M}_2$ from above endows \mathcal{M}_2 with the structure of an E_1 -module over the braid groupoid \mathcal{B} , and since the latter is braided monoidal, we can apply the results of [22] to study disk stabilization in \mathcal{M}_2 .

Remark 1.1. Homological stability frameworks such as [25, 22, 11] require an E_2 -algebra, or the weaker structure of E_1 -module over an E_2 -algebra, as input. This is a priori a lot of data, and it may be that the most natural choice in a given context simply does not admit an E_2 -structure. This turns out to be the case for the monoidal category of bidecorated surfaces \mathcal{M}_2 : In the context of categories, E_2 -structures are given by braided monoidal structures and we show in Section 5.3 that even the full monoidal subcategory of \mathcal{M}_2 generated by our stabilizing object, the disk D , does not admit a braiding. This distinguishes our situation from most previous examples of homological stability.

On the other hand, it does not take much to equip a given monoidal category \mathcal{X} with the structure of an E_1 -module over a braided monoidal category. In fact, as shown in Section 5.1, any Yang–Baxter operator in \mathcal{X} determines a strong monoidal functor $\mathcal{B} \rightarrow \mathcal{X}$ from the braid groupoid \mathcal{B} , and thus endows \mathcal{X} with the structure of an E_1 -module over \mathcal{B} . This perspective also makes sense if \mathcal{X} itself acts on a category \mathcal{M} , and one is interested in the stabilization

$$\mathcal{M} \xrightarrow{\oplus X} \mathcal{M} \xrightarrow{\oplus X} \dots$$

induced by acting with an object X of \mathcal{X} admitting a Yang–Baxter operator $\tau \in \text{Aut}_{\mathcal{X}}(X \oplus X)$. The category \mathcal{M} becomes this way likewise a module over \mathcal{B} , where the object n of \mathcal{B} acts on $A \in \mathcal{M}$ via $A \oplus n = A \oplus X^{\oplus n}$.

Disordered arcs Given a category \mathcal{M} as above, with the structure of an E_1 -module over a monoidal category \mathcal{X} with a distinguished Yang–Baxter operator (X, τ) , such that acting by X satisfies a certain injectivity property (see Proposition 3.4), the main result of [22] implies that homological stability for stabilization with X is controlled by the connectivity of certain *complexes of destabilizations*. In the category of bidecorated surfaces \mathcal{M}_2 , stabilizing with the bidecorated disk D corresponds homotopically to attaching an arc, and we show in Proposition 4.4 that the relevant complex of destabilizations for stabilizing a surface S with a disk n times identifies with the “disordered arc complex”¹ associated to the surface $S \# D^{\#n}$. This is a simplicial complex whose vertices are isotopy classes of non-separating arcs in the surface with endpoints $b_0 = I_0(1/2)$ and $b_1 = I_1(1/2)$, and where a collection of isotopy classes forms a simplex if the classes can be represented by arcs that are disjoint away from the endpoints, are jointly non-separating, and such that the arcs have the same ordering at I_0 and I_1 .

Writing $\mathcal{D}^\nu(S_{g,r}, b_0, b_1)$ for the disordered arc complex of a surface $S_{g,r}$ with marked points b_0 and b_1 in $\nu = 1$ or $\nu = 2$ boundary components, the main ingredient of our proof of homological stability is the following connectivity result:

Theorem C. (Theorem 2.5) The disordered arc complex $\mathcal{D}^\nu(S_{g,r}, b_0, b_1)$ is $\left(\frac{2g+\nu-5}{3}\right)$ -connected.

Remark 1.2. It is conjectured in [25, Conj C] that the complex of destabilizations is highly connected if and only if stability holds with all appropriate twisted coefficients. The slope $2/3$ bounds in Theorems A and B is precisely dictated by the same slope $2/3$ in Theorem C in the connectivity of the arc complex, which is the complex of destabilizations in that case. This connectivity bound is best possible among linear bounds as a better bound would prove an incorrect stability statement, see Remark 2.6.

¹We called those *disordered* arcs because it is the opposite ordering convention than the one used in the “ordered arc complex” of [24].

Organization of the paper. In Section 2 we prove the high connectivity of the disordered arc complex. In Section 3 we define the monoidal category of bidecorated surfaces $(\mathcal{M}_2, \#)$, as well as the action of the braid groupoid \mathcal{B} on this category. In Section 4, we show Theorems A and B by showing that the disordered arc complex agrees with the complex of destabilizations, and applying the main result of [22]. Finally, in Section 5 we explain the relationship between homological stability and Yang–Baxter operators, and show the non-braidedness of the category of bidecorated surfaces.

2. High connectivity of the disordered arc complex

In this section, we prove that the disordered arc complex is highly connected. It will be defined as a subcomplex of the following simplicial complex of non-separating arcs:

Definition 2.1. Let S be an orientable surface² with nonempty boundary, and let b_0, b_1 be distinct points in ∂S . The *complex of non-separating arcs* $\mathcal{B}(S, b_0, b_1)$ is the simplicial complex whose p -simplices are collections of $p+1$ distinct isotopy classes of arcs between b_0, b_1 that admit representatives a_0, \dots, a_p such that

- (a) $a_i \cap a_j = \{b_0, b_1\}$ for each $i \neq j$ and
- (b) $S - (a_0 \cup \dots \cup a_p)$ is connected.

For convenience, we will add a superscript $\mathcal{B}^\nu(S, b_0, b_1)$ to the notation of the complex, with $\nu = 1$ indicating that b_0, b_1 lie on the same boundary component and $\nu = 2$ indicating that they do not.

Note that an orientation of the surface defines orderings of the arcs a_0, \dots, a_p representing a simplex at both b_0 and b_1 . Reversing the orientation will also reverse the ordering of the arcs at both b_0 and b_1 , so it makes sense to define:

Definition 2.2. Let (S, b_0, b_1) be as before. The *disordered arc complex* is the subcomplex $\mathcal{D}^\nu(S_{g,r}, b_0, b_1) \subseteq \mathcal{B}^\nu(S, b_0, b_1)$ consisting of those simplices σ that admit arc representatives a_0, \dots, a_p , again subject to (a), (b), satisfying in addition

- (c) given an orientation of S , the induced ordering of the arcs at b_0 agrees with the induced ordering of the arcs at b_1 .

The definition of the disordered arc complex in fact also makes sense for non-orientable surfaces, given a chosen oriented arc around each of b_0 and b_1 (as will appear in Section 3), or equivalently for “oriented points” \vec{b}_0, \vec{b}_1 , as in [27], but we will here only consider oriented surfaces.

The name “disordered” was chosen to contrast with the pre-existing *ordered arc complex* used by Ivanov [18] in the case $\nu = 1$ and Randall-Williams [24] in their proofs of homological stability for the mapping class group of surfaces; the “ordered” version is also a subcomplex of the $\mathcal{B}^\nu(S, b_0, b_1)$, but with the requirement that the order of the arcs at b_1 is reversed compared to the order at b_0 . Fixing an ordering condition has the effect that the action of the mapping class group is transitive on the set of p -simplices for every p , see [14, Lem 3.2]. The ordered and disordered arc complexes represent the two extremes of how fast the genus of the surface

²By *surface* we mean a topological 2-manifold S which is compact except for a finite number of punctures, i.e. there is a compact topological 2-manifold \bar{S} and an embedding $i: S \hookrightarrow \bar{S}$ so that $\bar{S} \setminus i(S)$ is a (possibly empty) finite union of points.

decreases when cutting along larger and larger simplices: for the ordered arc complex, the genus goes down as fast as possible, essentially every time one removes an arc, while for the disordered arc complex, the genus goes down as slow as possible, i.e. only every other time. Before we can state this result, we must make the process of cutting away $\sigma \in \mathcal{B}^\nu(S, b_0, b_1)$ precise.

Construction 2.3. Given a simplex $\sigma \in \mathcal{B}^\nu(S, b_0, b_1)$, we will construct a new surface $S \setminus \sigma$ with marked points by cutting away σ and moving the marked points a little. In order to implement this construction, first pick representative arcs a_0, \dots, a_p satisfying conditions (a), (b), and (c) from above. Let $D_{\geq 0}^2 = \{z \mid |z| \leq 1, \operatorname{Re} z \geq 0\} \subset \mathbb{C}$ denote the half-disk, and pick disjoint charts $\varphi_i: D_{\geq 0}^2 \rightarrow S$ for $i = 0, 1$ compatible with orientation; that is, φ_i maps $D_{\geq 0}^2$ homeomorphically onto a closed neighborhood \bar{U}_i of $b_i = \varphi_i(0)$, whose interior we denote by U_i , and any orientation of S pulls back to the same orientation along φ_0 and φ_1 . Let $S' := S \setminus (U_1 \cup U_2)$ and pick disjoint tubular neighborhoods $T_i \supset a_i \cap S'$ in S' . Then we define

$$S \setminus \sigma := S' \setminus \left(\bigcup_{i=0}^p T_i \right).$$

We also define marked points $b'_i := \varphi_i(-i)$ to be the leftmost intersection of \bar{U}_i with ∂S . Although this construction depends on several choices, the triple $(S \setminus \sigma, b'_0, b'_1)$ is uniquely defined up to a homeomorphism that preserves the marked points.

If $\sigma \in \mathcal{D}^\nu(S, b_0, b_1)$, then there is a canonical injective map of simplicial complexes

$$(2.1) \quad \mathcal{D}^\mu(S \setminus \sigma, b'_0, b'_1) \longrightarrow \mathcal{D}^\nu(S, b_0, b_1)$$

given on a simplex $\langle [a'_0], \dots, [a'_q] \rangle$ by slightly spreading out the endpoints of the a'_j , so that they lie disjointly on the half-circles ∂U_i , and then radially extending each a'_j through U_i out to b_i , both at the endpoints corresponding to $i = 0$ and $i = 1$.

Proposition 2.4. For a p -simplex $\sigma = \langle [a_0], \dots, [a_p] \rangle \in \mathcal{D}^\nu(S_{g,r}, b_0, b_1)$, the cut surface $S_{g,r} \setminus \sigma$ has genus g' with r' boundary components for

$$g' = g - \left\lfloor \frac{p+3-\nu}{2} \right\rfloor \quad \text{and} \quad r' = \begin{cases} r - (-1)^\nu, & \text{if } p \text{ is even,} \\ r & \text{else.} \end{cases}$$

Proof. Let $S := S_{g,r}$. We first prove the formula for the number of boundary components. The proof is by induction on p . We may assume that the indices of a_0, \dots, a_p are compatible with the ordering at the endpoints b_0 and b_1 , so a_i lies before a_j at b_0 if and only if $i \leq j$. Note that by wiggling the representatives a_0, \dots, a_p a little, we may view a_0, \dots, a_{p-1} as defining a simplex in the disordered arc complex $\mathcal{D}^\mu(S \setminus \langle [a_p] \rangle, b'_0, b'_1)$ of the cut surface defined as above, where $\mu = 1$ if b'_0 and b'_1 lie on the same boundary component of $S \setminus \sigma$ and $\mu = 2$ else. By induction, it will therefore suffice to note that

- (i) the formula for the number of boundary components holds when $p = 0$, that is the number of boundary components of the surface increases by 1 if $\nu = 1$ and decreases by 1 if $\nu = 2$,
- (ii) $\mu = 3 - \nu$, i.e. $\mu = 1$ if $\nu = 2$ and vice-versa.

These two statements indeed imply in particular that cutting two arcs will recover both the original ν and the original r . The statements (i) and (ii) are local statements, and we refer to Figure 1 for their proof, where we note that, crucially, in the $\nu = 1$ case, the new marked points b'_0 and b'_1 lie on different boundary components of the cut surface.

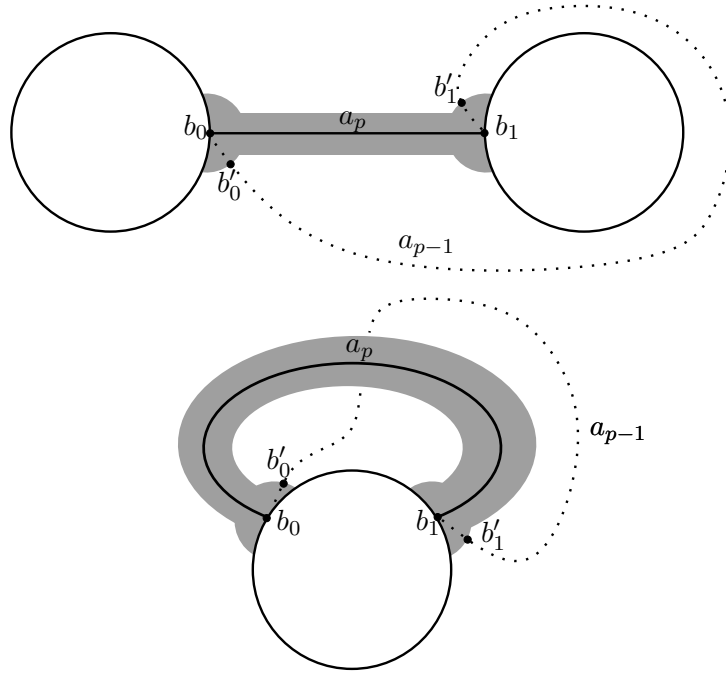


Figure 1: Effect of cutting an arc on the number of boundary components. The shaded area is the part of the surface that is removed when cutting along the arc a_p .

Now the Euler characteristic of the cut surface is $2 - 2g - r + p + 1 = 2 - 2g' - r'$. From this it follows that $g' = g - \frac{p+1-r+r'}{2}$. Hence for p odd we get $g' = g - \frac{p+1}{2}$ which one can check agrees with $g - \frac{p+1}{2} - \lfloor \frac{2-\nu}{2} \rfloor = g - \lfloor \frac{p+3-\nu}{2} \rfloor$ both when $\nu = 1$ and $\nu = 2$. When p is even, we get $g' = g - \frac{p+1-(-1)^\nu}{2} = g - \frac{p}{2} - \frac{1-(-1)^\nu}{2}$, and this again agrees with the given formula as $\frac{1-(-1)^\nu}{2} = \lfloor \frac{3-\nu}{2} \rfloor$ both with $\nu = 1$ and $\nu = 2$. \square

Note that the computation of the genus g' of the cut surface can also be seen as a special case of [6, Prop 2.11], applied to the case where the permutation α is the inversion $[p(p-1)\dots 0]$, once one computes that the genus $S(\alpha)$ of a neighborhood of the arcs is $\lfloor \frac{p+2-\nu}{2} \rfloor$, e.g. using Corollary 2.15 of the same paper.

The complex $\mathcal{B}^\nu(S, b_0, b_1)$ is known to be $(2g+\nu-3)$ -connected. (This was first stated in [14]; see [27, Thm 3.2] or [28, Thm 4.8] for a complete proof.) We will here use this fact to deduce that $\mathcal{D}^\nu(S_{g,r}, b_0, b_1)$ is also highly-connected. While the ordered arc complex is $(g-2)$ -connected [24, Thm A.1], the following result shows that the disordered arc complex is only slope $\frac{2}{3}$ connected with respect to the genus, despite being $\sim 2g$ -dimensional.

Theorem 2.5. *The disordered arc complex $\mathcal{D}^\nu(S_{g,r}, b_0, b_1)$ is $\left(\frac{2g+\nu-5}{3}\right)$ -connected.*

To prove the result, we use essentially the same argument as the one given in [24] in the ordered case.

Proof. Let $S = S_{g,r}$ and fix an orientation of S . In the case $g = 0$, the statement for $\mathcal{D}^1(S)$ is vacuous, and for $\mathcal{D}^2(S)$ it states that the complex is (-1) -connected, i.e. nonempty, which holds as any arc in the surface connecting b_0 and b_1 defines a vertex in $\mathcal{D}^2(S)$. We prove the remaining cases by induction on g .

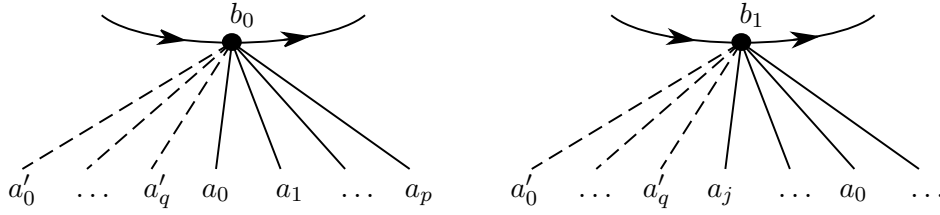


Figure 2: Maximal regular bad simplex $\{a_0, \dots, a_p\}$ and simplex $\{a'_0, \dots, a'_q\}$ in its link.

Let $g > 0$. Suppose we are given $f : \partial D^{k+1} \rightarrow \mathcal{D}^\nu(S, b_0, b_1)$ for some $k \leq (2g + \nu - 5)/3$. We wish to exhibit a nullhomotopy of this map. Since $(2g + \nu - 5)/3 \leq 2g + \nu - 3$, Theorem 3.2 in [27] enables us to choose a map \hat{f} such that the outer diagram

$$(2.2) \quad \begin{array}{ccc} \partial D^{k+1} & \xrightarrow{f} & \mathcal{D}^\nu(S, b_0, b_1) \\ \downarrow & \nearrow \text{dotted} & \downarrow \\ D^{k+1} & \xrightarrow{\hat{f}} & \mathcal{B}^\nu(S, b_0, b_1), \end{array}$$

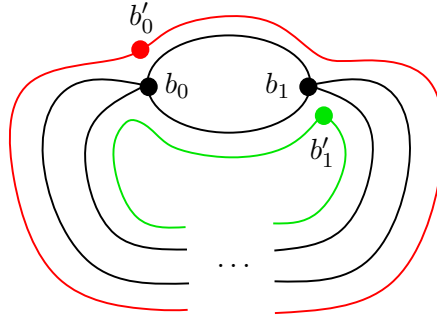
commutes. Using PL-approximation, we may assume that \hat{f} and f are simplicial with respect to some PL-triangulation of D^{k+1} . We will repeatedly replace \hat{f} until the dotted arrow exists, thereby giving the desired nullhomotopy.

Write $<_0$ and $<_1$ for the anti-clockwise orderings at b_0 and b_1 . We call a p -simplex σ in D^{k+1} *regular bad* if $\hat{f}(\sigma) = \langle [a_0], \dots, [a_p] \rangle$, indexed in such a way that $[a_0] <_0 \dots <_0 [a_p]$. and there is $j > 0$ with $[a_j] <_1 [a_0]$. Here $p' \leq p$ is the dimension of the image simplex $\hat{f}(\sigma)$, and $p' \geq 1$ if σ is regular bad. This condition is “dense” in the sense that any simplex σ in D^{k+1} with image not included in $\mathcal{D}^\nu(S, b_0, b_1)$ must contain a regular bad simplex as a face. Thus it suffices to give a procedure for exchanging \hat{f} with a map having strictly fewer regular bad simplices, while maintaining commutativity of the outer diagram (2.2).

Let σ be a regular bad simplex of D^{k+1} of maximal dimension p and consider its link $\text{Lk } \sigma \subset D^{k+1}$. Maximality of σ implies that $\hat{f}|_{\text{Lk } \sigma}$ factors as

$$\hat{f}|_{\text{Lk } \sigma} : \text{Lk } \sigma \rightarrow \mathcal{D}^\mu(S \setminus \hat{f}(\sigma), b'_0, b'_1) \rightarrow \mathcal{D}^\nu(S, b_0, b_1) \hookrightarrow \mathcal{B}^\nu(S, b_0, b_1),$$

where $(S \setminus \hat{f}(\sigma), b'_0, b'_1)$ is the cut surface defined in Construction 2.3 and the map in the middle is the canonical map (2.1). Indeed, suppose that $\tau \in \text{Lk } \sigma$ and write $\hat{f}(\tau) = \langle [a'_0], \dots, [a'_q] \rangle$. If $[a_0] \leq_0 [a'_i]$ for any i , then the simplex $\sigma * v$ is regular bad of a larger dimension than σ for any vertex $v \in \tau$ with $\hat{f}(v) = [a'_i]$, contradicting maximality. So we must have $[a'_i] <_0 [a_0]$ for each i , and hence the arcs $a_i \cap (S \setminus \hat{f}(\sigma))$ start at the boundary component containing b'_0 . Now we must also have that each $[a'_i] <_1 [a_0]$ as otherwise $\sigma * v$ would again be regular bad for any lift v of $[a'_i]$. Thus we can view $\langle [a'_0], \dots, [a'_q] \rangle$ as a simplex in $\mathcal{B}^\mu(S \setminus \hat{f}(\sigma), b'_0, b'_1)$ by intersecting with $S \setminus \hat{f}(\sigma)$ and sliding endpoints slightly so they are all at b'_0 and b'_1 . Finally, we must see that under this identification $\langle [a'_0], \dots, [a'_q] \rangle$ lies in the subcomplex $\mathcal{D}^\mu(S \setminus \hat{f}(\sigma), b'_0, b'_1)$, which is now equivalent to showing that $\langle [a'_0], \dots, [a'_q] \rangle \in \mathcal{D}^\nu(S, b_0, b_1)$, as the ordering does not change under the small radial extension that translates between these disordered arc complexes. But supposing for contradiction that there is i and j with $[a'_i] <_0 [a'_j]$ with $[a'_j] <_1 [a'_i]$, then picking lifts $\hat{f}(v) = [a'_i]$ and $\hat{f}(w) = [a'_j]$, we find that $\sigma * \langle v, w \rangle$ would again be regular bad of larger dimension than σ . Thus $\hat{f}(\tau)$ must be disordered, showing that we have the desired factorization.


 Figure 3: Regular bad 1-simplex with $\nu = 1$.

The link $\text{Lk}(\sigma)$ is a simplicial sphere $S^{k-p} \subset D^{k+1}$. We want to show that the map $\hat{f}|_{\text{Lk}(\sigma)}$ extends to a simplicial map

$$(2.3) \quad F : D^{k-p+1} \longrightarrow \mathcal{D}^\mu(S \setminus \hat{f}(\sigma), b'_0, b'_1) \longrightarrow \mathcal{D}^\nu(S, b_0, b_1) \hookrightarrow \mathcal{B}(S, b_0, b_1)$$

for D^{k-p+1} a disk with some PL-structure extending that of $\text{Lk}(\sigma)$. This will follow if we can show that the complex $\mathcal{D}^\mu(S \setminus \hat{f}(\sigma), b'_0, b'_1)$ is $(k-p)$ -connected. Note that we necessarily have $g(S \setminus \hat{f}(\sigma)) < g$ as $f(\sigma)$ is a non-separating p' -simplex with $p' \geq 1$. Hence we can use our induction hypothesis. We consider the cases $\nu = 1$ and $\nu = 2$ separately.

Case 1: $\nu = 1$. We have that $g(S \setminus \hat{f}(\sigma)) \geq g - p' - 1 \geq g - p - 1$, as removing $p' + 1$ arcs reduces the genus by at most $p' + 1 \leq p + 1$. Hence by induction we have that $\mathcal{D}^\mu(S \setminus \hat{f}(\sigma), b'_0, b'_1)$ is $(\frac{2(g-p-1)-4}{3})$ -connected, using also that $\mu \geq 1$. If $p \geq 2$, we have

$$k - p \leq \frac{2g - 4}{3} - p = \frac{2g - 3p - 4}{3} \leq \frac{2(g - p - 1) - 4}{3}.$$

For $p = p' = 1$, note that b'_0, b'_1 necessarily lie in different boundary components, so that $\mu = 2$ in that case. (See Figure 3.) Hence in that case $\mathcal{D}^\mu(S \setminus \hat{f}(\sigma), b'_0, b'_1)$ is $(\frac{2(g-2)-3}{3})$ -connected, and

$$k - 1 \leq \frac{2g - 4}{3} - 1 = \frac{2g - 7}{3} = \frac{2(g - 2) - 3}{3}.$$

so we get the desired extension in both subcases.

Case 2: $\nu = 2$. The fact that b_0, b_1 lie in different components implies that

$$g(S \setminus \hat{f}(\sigma)) \geq g - p' \geq g - p$$

as cutting along the first arc has no effect on the genus. Hence induction here gives that $\mathcal{D}^\mu(S \setminus \hat{f}(\sigma), b'_0, b'_1)$ is $(\frac{2(g-p)-4}{3})$ -connected. Now for all $p \geq 1$,

$$k - p \leq \frac{2g - 3}{3} - p = \frac{2g - 3p - 3}{3} \leq \frac{2(g - p) - 4}{3}$$

yielding the desired connectivity.

We will use the map F of (2.3) to modify \hat{f} in the star $\text{St}(\sigma)$. For this purpose, note that as simplicial subcomplexes of D^{k+1} ,

$$\begin{aligned} \text{St}(\sigma) &= \sigma * \text{Lk}(\sigma), \\ \partial \text{St}(\sigma) &= \partial \sigma * \text{Lk}(\sigma). \end{aligned}$$

In particular, we get an identification $\partial(\partial\sigma * D^{k-p+1}) \cong \partial\text{St}(\sigma)$ for D^{k-p+1} the simplicial disk that is the source of the map F above.

We replace $\hat{f}|_{\text{St}(\sigma)}$ by the unique simplicial map

$$\hat{f} * F : \partial\sigma * D^{k-p+1} \longrightarrow \mathcal{B}^\nu(S, b_0, b_1).$$

It remains to show that this has improved the situation. Indeed, suppose that $\tau = \tau_0 * \tau_1$ is a regular bad simplex in $\partial\sigma * D^{k-p+1}$. By construction, τ_1 has image in $\mathcal{D}^\mu(S \setminus \hat{f}(\sigma), b'_0, b'_1) \subset \mathcal{D}^\nu(S, b_0, b_1)$, so the ordering of the arcs of τ at b_0 and b_1 starts with the arcs of τ_1 , all in anti-clockwise order. Hence, if τ is regular bad, we must have that $\tau = \tau_0$ is a strict face of σ . In particular, no new regular bad simplices have been added. As the simplex σ has been removed, we have thus reduced the total number of regular bad simplices in the disk. Repeating this procedure, we will after finitely many stages remove every regular bad simplex, thus making the dashed arrow exist, which proves the result. \square

Remark 2.6. The connectivity estimate above can be shown to be optimal in certain low-genus examples, corresponding to known computations of the unstable homology of mapping class groups. Indeed, $\mathcal{D}^2(S_{1,r})$ is disconnected. To see this, consider the spectral sequence associated to the action of the mapping class group $\Gamma(S_{1,r})$ on the simplicial complex $\mathcal{D}^2(S_{1,r})$. This is the spectral sequence arising from the vertical filtration of the double complex $\mathbb{Z}\mathcal{D}^2(S_{1,r})_\bullet \otimes_{\Gamma(S_{1,r})} F_\bullet$, where $F_\bullet \rightarrow \mathbb{Z}$ is a free resolution of the trivial $\Gamma(S_{1,r})$ -module. By a standard argument using Shapiro’s lemma (see e.g. [17, Thm 5.1] or [16, Sec 1]), one finds that the first page of this spectral sequence is given by

$$E_{p,q}^1 \cong \begin{cases} \tilde{H}_q(\Gamma(S_{1,r})) & \text{if } p = -1, \\ \tilde{H}_q(\Gamma(S_{1,r-1})) & \text{if } p = 0, \\ \tilde{H}_q(\Gamma(S_{0,r})) & \text{if } p = 1, \\ \tilde{H}_q(\Gamma(S_{0,r-1})) & \text{if } p = 2, \\ 0 & \text{otherwise.} \end{cases}$$

Assume for contradiction that $\mathcal{D}^2(S_{1,r})$ is connected. Then an analysis of the horizontal filtration of the double complex $\mathbb{Z}\mathcal{D}^2(S_{1,r})_\bullet \otimes_{\Gamma(S_{1,r})} F_\bullet$ shows that $E_{p,q}^\infty = 0$ for $p + q \leq 0$, so the differential $d^1 : H_1(\Gamma(S_{1,r-1})) \rightarrow H_1(\Gamma(S_{1,r}))$ must be surjective. This contradicts the fact that $H_1(\Gamma(S_{1,s})) \cong \mathbb{Z}^s$ for $s \geq 1$ (see [21, Thm 5.1]). Hence it is not true that \mathcal{D}^ν is $\left(\frac{2g+\nu-4}{3}\right)$ -connected when $\nu = 2$.

Similarly, one finds that $H_1(\mathcal{D}^1(S_{3,r})) \neq 0$ by considering the spectral sequence associated to the action of $\Gamma(S_{3,r})$ on $\mathcal{D}^1(S_{2,r+1})$ and noting that the differential $d^1 : H_1(\Gamma(S_{2,r+1})) \rightarrow H_1(\Gamma(S_{3,r}))$ cannot be injective since the source identifies with $\mathbb{Z}/10\mathbb{Z}$ and the target is zero (see [21, Thm 5.1]). Thus \mathcal{D}^ν fails to be $\left(\frac{2g+\nu-4}{3}\right)$ -connected when $\nu = 1$ also.

Note that these low dimensional computations also show that the first and last ranges in Theorem A cannot be improved by a constant.

3. The monoidal category of bidecorated surfaces

In this section, we describe a monoidal groupoid $(\mathcal{M}_2, \#)$ of surfaces decorated by two intervals in their boundary, where the monoidal structure glues the intervals in pairs. We show that this groupoid is a module over the braided monoidal groupoid \mathcal{B} of braid groups, giving, on classifying spaces, the structure of an E_1 -module over an E_2 -algebra in the sense of [22].

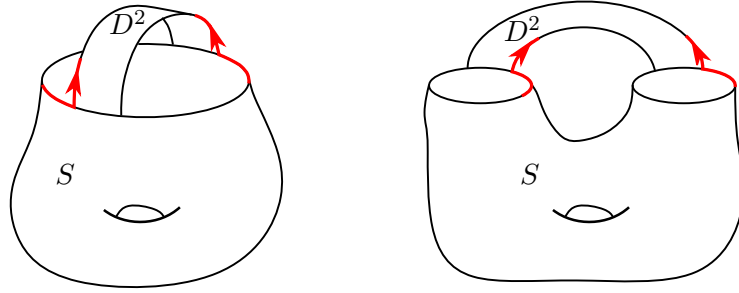


Figure 4: Gluing a disk $X_1 = D^2$ to a bidecorated surface S

3.1 Bidecorated surfaces and the monoidal structure The groupoid \mathcal{M}_2 has objects *bidecorated surfaces*, that are, informally, surfaces with two intervals marked in their boundary. To give a precise definition of the objects that is convenient for the monoidal structure, we start by constructing a special sequence of bidecorated surfaces X_n , built out of disks, and defined inductively.

Let $X_1 = D^2 \subset \mathbb{C}$ denote the unit disk in the complex plane, and define the embeddings $\iota_1^0, \iota_1^1: I \rightarrow X_1$ by

$$\iota_1^0(t) = e^{i(\pi/4+t\pi/2)} \quad \text{and} \quad \iota_1^1(t) = e^{i(5\pi/4+t\pi/2)}.$$

We denote by $\overline{\iota_1^i}: I \rightarrow X_1$ the reversed map $t \mapsto \iota_1^i(1-t)$ for $i = 0, 1$.

Recursively, suppose we have defined $(X_m, \iota_m^0, \iota_m^1)$ for some $m \geq 1$. We construct X_{m+1} from X_m by gluing an additional disk along two half intervals, with new markings $\iota_{m+1}^0, \iota_{m+1}^1$ coming from the first half of the markings of X_m and the second half of the markings of the attached disk:

$$X_{m+1} := \frac{X_m \sqcup X_1}{\iota_m^i(t) \sim \overline{\iota_1^i}(t), t \in [1/2, 1]}, \quad \text{with} \quad \iota_{m+1}^i(t) = \begin{cases} \iota_m^i(t), & \text{if } t \leq 1/2, \\ \iota_1^i(t), & \text{else.} \end{cases}$$

for $i = 0, 1$. Note that the marked intervals in the boundary of X_m might live in different boundary components (in fact this will happen every other time). Figure 4 shows what happens when a disk is glued to a surface in the above described manner, in each of these two possible cases.

Lemma 3.1. *Let $m \geq 1$. Then X_m is an orientable surface of genus g with r boundary components, where*

$$(g, r) = \begin{cases} (\frac{m}{2} - 1, 2), & \text{if } m \text{ is even,} \\ (\frac{m-1}{2}, 1), & \text{if } m \text{ is odd.} \end{cases}$$

Proof. Note first that X_m is a connected orientable surface for each m , since X_1 is a disk and X_m is obtained from X_1 by successively adding disks (or strips), attached along two disjoint intervals in the boundary. For the same reason, we get that the Euler characteristic of X_m is

$$\chi(X_m) = \chi(X_{m-1}) - 1 = \dots = 2 - m.$$

By the classification of surfaces, we are left to compute the number of boundary components of X_m . For this, observing Figure 4, we notice that if we glue a disk along two intervals of S that lie in the same boundary component, the new marked intervals given by the above procedure will give new intervals in different boundary components and vice versa, and no boundary component

without marked intervals are ever created. It follows that the number of boundary components of X_m alternates between 1 and 2. The result follows. \square

We are now ready to define the objects of the groupoid \mathcal{M}_2 . We will use the boundary of the above defined surfaces X_m to parametrize the boundary components of the surfaces that contain the marked intervals, to allow us to work with parametrized boundary components instead of parametrized arcs, in order to simplify some definitions.

Definition 3.2. A *bidecorated surface* is a tuple (S, m, φ) where S is a surface, $m \geq 1$ is an integer, and

$$\varphi: \partial X_m \sqcup (\sqcup_k S^1) \xrightarrow{\sim} \partial S$$

is a homeomorphism, giving a parametrization of the boundary of S . We think of (S, m, φ) as a surface with two parametrized arcs

$$I_0 := \varphi \circ \iota_m^0 \quad \text{and} \quad I_1 := \varphi \circ \iota_m^1$$

in its boundary, and k additional parametrized boundaries. The surface S may also have punctures.

The monoidal groupoid $(\mathcal{M}_2, \#, U)$ has objects the bidecorated surfaces together with a formal unit U . There are no morphisms between two bidecorated surfaces (S, m, φ) and (S', m', φ') unless S and S' are homeomorphic and $m = m'$, in which case we define the set of morphisms to be all the mapping classes of homeomorphisms that preserve the boundary parametrizations

$$\text{Hom}_{\mathcal{M}_2}((S, m, \varphi), (S', m, \varphi')) := \pi_0 \text{Homeo}_{\partial}(S, S') = \pi_0 \{f \in \text{Homeo}(S, S') \mid f \circ \varphi = \varphi'\},$$

where $\text{Homeo}(S, S')$ is endowed with the compact-open topology, and $\text{Homeo}_{\partial}(S, S')$ with the subspace topology. The only morphism involving the unit U is the identity id_U .

Remark 3.3. Our definition of the morphisms in the category \mathcal{M}_2 is such that punctures in a surfaces S can be permuted by automorphisms of S in \mathcal{M}_2 . Our argument works just as well with labeled punctures, that are not permutable by homeomorphisms, or both labeled and unlabeled punctures, just like we could also have additional boundary components that are only marked up to a permutation. The only changes this would cause to the argument would be that it would make the notations and conventions more cumbersome.

The monoidal structure $\#$ is defined as follows. The object U is by definition a unit for $\#$. For the remaining objects, the monoidal product $\#$ is defined by

$$(S, m, \varphi) \# (S', m', \varphi') := \left(\frac{S \sqcup S'}{I_i(t) \sim \overline{I'_i}(t) \text{ for } t \in [1/2, 1], i \in \{0, 1\}}, m + m', \varphi \# \varphi' \right),$$

where $\overline{I'_i}$ denotes the reversed arc $t \mapsto I'_i(1 - t)$, and where

$$\varphi \# \varphi': \partial X_{m+m'} \sqcup (\sqcup_{k+k'} S^1) \hookrightarrow \partial(S \# S'),$$

is obtained using the canonical identification $\partial X_{m+m'} \cong (\partial X_m \setminus \iota_m(\frac{1}{2}, 1)) \cup (\partial X_{m'} \setminus \iota_{m'}(0, \frac{1}{2}))$. On morphisms, the monoidal product is given by juxtaposition.

The monoidal category \mathcal{M}_2 has the following *injectivity property* with respect to gluing a disk, which will be useful in the proof of our stability result.

Proposition 3.4. *For any object $S = (S, m, \varphi)$ of \mathcal{M}_2 , and any $p \geq 0$, the map*

$$\text{Aut}_{\mathcal{M}_2}(S) \xrightarrow{\#D^{\#p+1}} \text{Aut}_{\mathcal{M}_2}(S \# D^{\#p+1})$$

is injective, where $D = (X_1, 1, \text{id})$ is our chosen disk.

Proof. Recall that the underlying surface of $D^{\#p+1}$ is the surface X_{p+1} defined above. Picking a smooth representative of the underlying surface of $S \# X_{p+1}$, with S a smooth subsurface in its interior, we can model the map in the statement using the description of the mapping class group of surfaces in terms of isotopy classes of diffeomorphisms rather than homeomorphisms. (See e.g., [5, Thm 1.2] for a detailed account of the classical isomorphism $\pi_0 \text{Homeo}_{\partial}(S) \cong \pi_0 \text{Diff}_{\partial}(S)$ when S is compact.) Now the result follows by essentially the same argument as the case of attaching of surface along a single arc instead of two, as treated in [25, Prop 5.18], using the fibration

$$\begin{aligned} \text{Diff}(S \# X_{p+1} \text{ rel } \partial S \cup X_{p+1}) &\longrightarrow \text{Diff}(S \# X_{p+1} \text{ rel } \partial(S \# X_{p+1})) \\ &\longrightarrow \text{Emb}((X_{p+1}, I_0|_{[\frac{1}{2}, 1]} \cup I_1|_{[\frac{1}{2}, 1]}), (S \# X_{p+1}, I_0|_{[\frac{1}{2}, 1]} \cup I_1|_{[\frac{1}{2}, 1]})) \end{aligned}$$

where the fiber identifies with $\text{Diff}(S \text{ rel } \partial_0 S)$ and where we note that $I_0|_{[\frac{1}{2}, 1]} \cup I_1|_{[\frac{1}{2}, 1]} = \partial X_{p+1} \cap \partial(S \# X_{p+1})$. Injectivity of the first map on π_0 follows if we can show that the base is simply-connected. In fact the base can be shown inductively to have contractible components, using that X_{p+1} is built inductively by attaching disks along two intervals, or homotopically attaching arcs, and using the contractibility of the components of embeddings of arcs in a surface, as proved in [12, Thm 5]. □

3.2 Braided action We want to apply the homological stability machine of [22] to stabilization in \mathcal{M}_2 with the bidecorated disk

$$D := (X_1, 1, \text{id}).$$

For this, we need that the classifying space of \mathcal{M}_2 is an E_1 -module over an E_2 -algebra. This will follow if we can show on the categorical level that \mathcal{M}_2 admits an appropriate action of a braided monoidal groupoid. We will build such an action in this section, using as braided monoidal groupoid the groupoid of braid groups. In contrast with most classical examples of homological stability, we will show in Section 5.3 that this action of the braid groupoid does not come from a braided structure on \mathcal{M}_2 , or the full monoidal subcategory generated by D . It is instead constructed using a *Yang–Baxter element* in \mathcal{M}_2 , associated to a braid subgroup of the mapping class group of X_m , that we will describe now.

Write

$$D^{\#m} = D_1 \# \dots \# (D_i \# D_{i+1}) \# \dots \# D_m,$$

where we use subscripts to enumerate the disks, and where the underlying surface is X_m . We let a_i denote the isotopy class of a curve in the interior $D_i \# D_{i+1} \cong S^1 \times I$ that is parallel to its boundary components, as shown in Figure 5.

Lemma 3.5. *The curves a_1, \dots, a_{m-1} form a chain in $D^{\#m}$, i.e. a_i and a_{i+1} have intersection number 1 for each i , and $a_i \cap a_j = \emptyset$ if $|i - j| > 1$.*

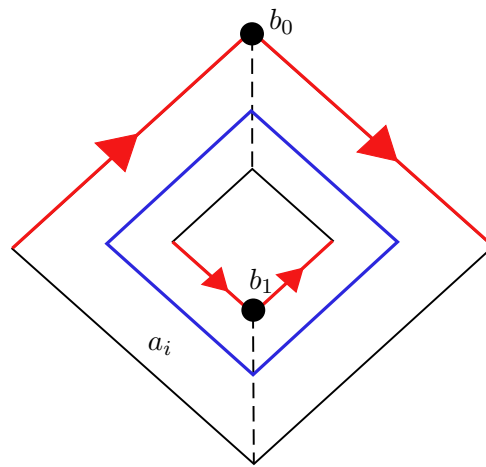


Figure 5: The curve a_i in $D_i \# D_{i+1}$

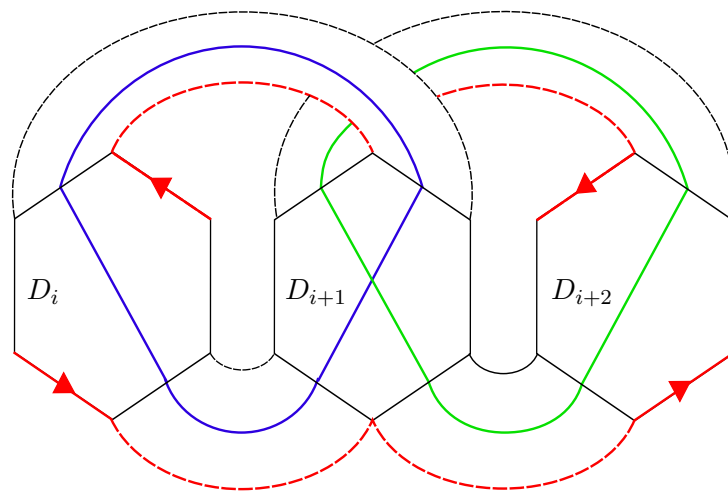


Figure 6: Intersection of a_i (blue) and a_{i+1} (green) in the underlying surface of $D_i \# D_{i+1} \# D_{i+2}$. The dashed strips indicate which edges are identified.

Proof. The curve a_i lives in the disks D_i and D_{i+1} , so it can only intersect a_{i-1} and a_{i+1} non-trivially, and hence it suffices to consider the subsurface of $D^{\#m}$ corresponding to $D_i \# D_{i+1} \# D_{i+2}$. Here the claim can be checked by hand, see Figure 6. \square

Let $T_i \in \text{Aut}_{\mathcal{M}_2}(D^{\#m})$ denote the Dehn twist³ along the curve a_i in $D^{\#m}$. A classical fact states that the Dehn twists along a chain of embedded curves satisfy the braid relations (see e.g. [9, 3.9 and 3.11]):

$$(3.1) \quad \begin{aligned} T_i T_{i+1} T_i &= T_{i+1} T_i T_{i+1} && \text{for all } i, \\ T_i T_j &= T_j T_i && \text{if } |i - j| > 1, \end{aligned}$$

Note that the same relations are satisfied by the inverse twists T_i^{-1} , which will turn out to be more convenient for us. Also, adding a disk to the right or left of $D^{\#m}$ gives the relations

$$T_i \# \text{id}_D = T_i \quad \text{and} \quad \text{id}_D \# T_i = T_{i+1}$$

in $\text{Aut}_{\mathcal{M}_2}(D^{\#m+1})$. In particular (3.1) includes the relation

$$(T_1^{-1} \# \text{id}_D)(\text{id}_D \# T_1^{-1})(T_1^{-1} \# \text{id}_D) = (\text{id}_D \# T_1^{-1})(T_1^{-1} \# \text{id}_D)(\text{id}_D \# T_1^{-1})$$

in $\text{Aut}_{\mathcal{M}_2}(D^{\#3})$, so in other words, the inverse Dehn twist $T_1^{-1} \in \text{Aut}_{\mathcal{M}_2}(D \# D)$ defines a Yang–Baxter operator in the sense of Section 5.1.

Recall from the introduction that \mathcal{B} denotes the monoidal groupoid of braid groups, with objects the natural numbers $\{0, 1, 2, \dots\}$, automorphisms of n the braid group B_n , and no other non-trivial morphisms. In Section 5.1 we show that, being a Yang–Baxter operator, the pair (D, T_1^{-1}) yields a strong monoidal functor

$$\Phi = \Phi_{D, T_1^{-1}} : (\mathcal{B}, \oplus) \longrightarrow (\mathcal{M}_2, \#),$$

uniquely determined up to monoidal natural isomorphism by the fact that $\Phi(1) = D$ and, for the standard generator $\sigma_1 \in B_2 = \text{Aut}_{\mathcal{B}}(1)$, $\Phi(\sigma_1) = T_1^{-1}$.

Such a functor Φ endows \mathcal{M}_2 with the structure of an E_1 -module over \mathcal{B} via the associated functor

$$\alpha = (- \# \Phi(-)) : \mathcal{M}_2 \times \mathcal{B} \longrightarrow \mathcal{M}_2,$$

given on objects by $\alpha(S, n) = S \# \Phi(n) = S \# D^{\#n}$, and likewise for morphisms. On classifying spaces, this yields exactly the kind of input needed in Krannich’s homological stability framework, see [22, Lem 7.2].

Remark 3.6. For each m , the restriction of the functor $\Phi : \mathcal{B} \longrightarrow \mathcal{M}_2$ to $B_m = \text{Aut}_{\mathcal{B}}(m)$ maps the standard generator σ_i to the inverse Dehn twist $T_i^{-1} \in \text{Aut}_{\mathcal{M}_2}(D^{\#m}) = \pi_0 \text{Homeo}_{\partial}(X_m)$. By Birman–Hilden theory [3, 4] the homomorphisms $\Phi|_{B_m} : B_m \longrightarrow \text{Aut}_{\mathcal{M}_2}(D^{\#m})$ are actually injective.

³In this article, “Dehn twist” always means right-handed Dehn twist.

4. Homological stability

Generalizing the main result of [25], Krannich associates to an E_1 -module \mathbf{M} over an E_2 -algebra \mathbf{X} in spaces together with a chosen stabilizing object $X \in \mathbf{X}$, a *space of destabilizations* at every $A \in \mathbf{M}$, whose high connectivity implies homological stability at A when stabilizing by X . We are interested in the case where $\mathbf{M} = B\mathcal{M}_2$ is the classifying space of \mathcal{M}_2 and $\mathbf{X} = B\mathcal{B}$, acting on $B\mathcal{M}_2$ via the map induced by the functor $\alpha: \mathcal{M}_2 \times \mathcal{B} \rightarrow \mathcal{M}_2$ defined in Section 3.2. We will pick $A = S \in \mathcal{M}_2$ to be some surface, with $X = 1 \in \mathcal{B}$ modelling stabilization with the disk as $\alpha(-, X) = - \# D$ is the sum with the bidecorated disk $D = (X_1, 1, \text{id})$ of Section 3.1.

Generally, the space of destabilizations is a semi-simplicial space, but in settings such as ours, it is actually levelwise homotopy discrete. Indeed, by [22, Lem 7.6]), when the structure of E_1 -module over an E_2 -algebra is induced by an action of a braided monoidal category on a groupoid, and under the injectivity condition given in Proposition 3.4, the space of destabilizations is equivalent to the following semi-simplicial set, defined just as in [25] in the case of a braided monoidal groupoid acting on itself.

Definition 4.1. ([22, Def 7.5]) Let (\mathcal{M}, \oplus) be a right module over a braided monoidal groupoid (\mathcal{X}, \oplus, b) , where we denote also by \oplus the module action. Let A and X be objects of \mathcal{M} and \mathcal{X} respectively. The *space of destabilizations* $W_n(A, X)_\bullet$ is the semi-simplicial set with set of p -simplices

$$W_n(A, X)_p = \{(B, f) \mid B \in \text{Ob}(\mathcal{M}) \text{ and } f: B \oplus X^{\oplus p+1} \rightarrow A \oplus X^{\oplus n} \text{ in } \mathcal{M}\} / \sim$$

where $(B, f) \sim (B', f')$ if there exists an isomorphism $g: B \rightarrow B'$ in \mathcal{C} satisfying that $f = f' \circ (g \oplus \text{id}_{X^{\oplus p+1}})$. The face map $d_i: W_n(A, X)_p \rightarrow W_n(A, X)_{p-1}$ is defined by $d_i[B, f] = [B \oplus X, d_i f]$ for

$$d_i f: B \oplus X \oplus X^p \xrightarrow{\text{id}_B \oplus b_{X^{\oplus i}, X}^{-1} \oplus \text{id}_{X^{\oplus p-i}}} B \oplus X^{\oplus i} \oplus X \oplus X^{\oplus p-i} \xrightarrow{f} A \oplus X^{\oplus n},$$

for $b_{X^{\oplus i}, X}^{-1}: X \oplus X^{\oplus i} \rightarrow X^{\oplus i} \oplus X$ coming from the braiding in \mathcal{X} .

4.1 Disk destabilizations and disordered arcs Given a bidecorated orientable surface $S = (S, m, \varphi)$, with I_0, I_1 compatibly oriented, let $\mathcal{D}(S) = \mathcal{D}^\nu(S, b_0, b_1)$ denote the disordered arc complex of S as in Section 2, where

$$b_0 = I_0(1/2) \quad \text{and} \quad b_1 = I_1(1/2)$$

are the midpoints of the marked intervals, $\nu = 1$ if I_0 and I_1 lie on the same boundary component, and $\nu = 2$ otherwise. The vertices of a simplex in $\mathcal{D}(S)$ are canonically ordered by the anti-clockwise ordering at b_0 (or equivalently at b_1). Hence we can associate to this simplicial complex a semi-simplicial set that we denote $\mathcal{D}(S)_\bullet$, with same set of p -simplices and whose i th face map is given by forgetting the $(i + 1)$ st arc with respect to that ordering. As $\mathcal{D}(S)$ and $\mathcal{D}(S)_\bullet$ have homeomorphic realizations, they have the same connectivity.

Write $W_n(S, D)_\bullet$ for the space of destabilizations of Definition 4.1 associated to the module $\mathcal{M} = \mathcal{M}_2$ over the braided monoidal groupoid $\mathcal{X} = \mathcal{B}$ acting on \mathcal{M}_2 as above, with $X = 1 \in \mathcal{B}$, and $A = S = (S_{g,r}^s, m, \varphi)$ some bidecorated orientable surface of small genus $g \geq 0$, with r boundary components and s punctures. The space $W_n(S, D)_\bullet$ is then the space of destabilizations of the stabilization map

$$\text{Aut}_{\mathcal{M}_2}(S \# D^{\#n-1}) \xrightarrow{\#D} \text{Aut}_{\mathcal{M}_2}(S \# D^{\#n})$$

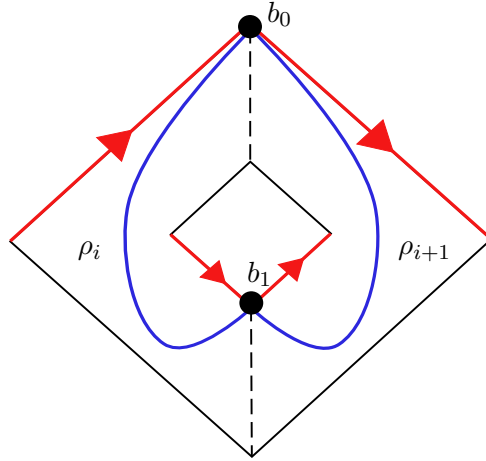


Figure 7: Ordering of the arcs ρ_i at their endpoints

that attaches an additional disk to the surface along the two marked intervals.

We want to identify $W_n(S, D)_\bullet$ with $\mathcal{D}(S \# D^{\#n})_\bullet$. For this, we start by constructing a particular disordered collection of arcs in $D^{\#n}$. Write again

$$D^{\#n} = D_1 \# \dots \# D_i \# \dots \# D_n,$$

and let ρ_i denote the unique isotopy class of arc in the i th disk D_i going from $b_0 = I_0(1/2)$ to $b_1 = I_1(1/2)$.

Lemma 4.2. *The arcs ρ_1, \dots, ρ_m are ordered anti-clockwise at both b_0 and b_1 .*

Proof. It suffices to show that ρ_i and ρ_{i+1} are ordered anti-clockwise at b_0 and b_1 for each i . Thus we need only consider what happens in the subsurface $D_i \# D_{i+1}$. The gluing being defined in exactly the same way at I_0 and I_1 , the arcs are ordered in the same way at both endpoints, and the particular choice of gluing gives the anti-clockwise ordering, see Figure 7. \square

Recall from Section 3.2 the Dehn twist T_i along the curve a_i in $D_i \# D_{i+1}$. The union of the arcs ρ_i in $D^{\#m}$ define a deformation retract of the surface, as each disk D_i retracts onto the corresponding arc ρ_i , and we can understand the action of the twists T_i on the surface by considering their action on the arcs ρ_i . Below we will need a description of this action in order to compare the face maps in the semi-simplicial sets $W_n(S, D)_\bullet$ with $\mathcal{D}(S \# D^{\#n})_\bullet$.

Lemma 4.3. *The action of the Dehn twist T_i along the curve a_i on the homotopy classes of the arcs ρ_i , relative to their endpoints, is*

$$T_i(\rho_j) = \begin{cases} \rho_i \rho_{i+1}^{-1} \rho_i & \text{if } j = i, \\ \rho_i & \text{if } j = i + 1, \\ \rho_j & \text{else,} \end{cases}$$

where we compose and invert homotopy classes of arcs relative to their endpoints by viewing them as elements in the fundamental groupoid of $S \# D^{\#n}$. Equivalently,

$$T_i^{-1}(\rho_i) = \rho_{i+1} \quad \text{and} \quad T_i^{-1}(\rho_{i+1}) = \rho_{i+1} \rho_i^{-1} \rho_{i+1}$$

and T_i^{-1} leaves the other ρ_j invariant.

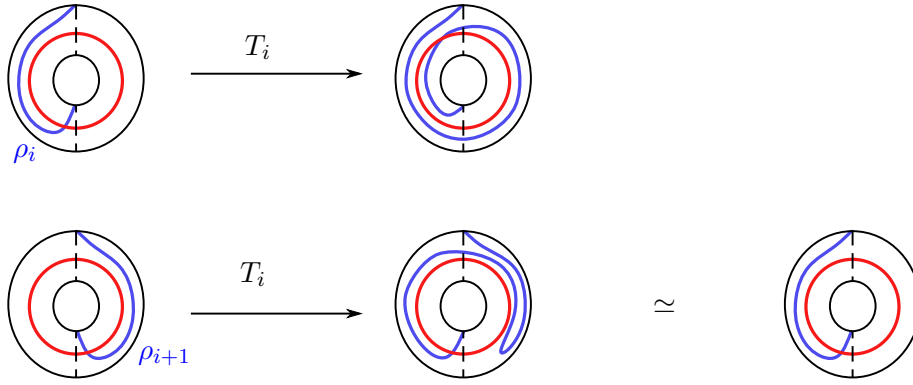


Figure 8: The action of the Dehn twist T_i on the arcs ρ_i (top) and ρ_{i+1} (bottom)

Proof. The Dehn twist T_i can only affect ρ_i and ρ_{i+1} as the curve a_i only intersects these two arcs, from which the last case in the statement follows. The computation for the arcs ρ_i and ρ_{i+1} is local to $D_i \# D_{i+1}$, where, as shown in Figure 8, we have $T_i(\rho_i) \simeq \rho_i \rho_{i+1}^{-1} \rho_i$, giving the first case in the statement, and $T_i(\rho_{i+1}) \simeq \rho_i$, giving the second case. \square

Proposition 4.4. *Let $S = (S, m, \varphi)$ be an object of \mathcal{M}_2 . There is an isomorphism of semi-simplicial sets*

$$W_n(S, D)_\bullet \cong \mathcal{D}^\nu(S \# D^{\#n})_\bullet$$

where the marked points b_0 and b_1 are the midpoints of the intervals I_0 and I_1 in $S \# D^{\#n}$ and with $\nu = \text{parity}(m+n)$, that is $\nu = 1$ if I_0 and I_1 lie in the same boundary component of $S \# D^{\#n}$ and $\nu = 2$ otherwise.

Proof. We first demonstrate that both $W_n(S, D)_p$ and $\mathcal{D}^\nu(S \# D^{\#n})_p$ are isomorphic, as sets with $\text{Aut}_{\mathcal{M}_2}(S \# D^{\#n})$ -actions, to $\text{Aut}_{\mathcal{M}_2}(S \# D^{\#n}) / \text{Aut}_{\mathcal{M}_2}(S \# D^{\#n-p-1})$ for every $p \geq 0$. This holds by definition for the first semi-simplicial set. For $\mathcal{D}^\nu(S \# D^{\#n})_p$, it will follow from two facts: (1) the natural action of

$$\text{Aut}_{\mathcal{M}_2}(S \# D^{\#n}) = \pi_0 \text{Homeo}_\partial(S \# D^{\#n})$$

on this set of p -simplices is transitive, and (2) the stabilizer of a p -simplex is isomorphic to $\text{Aut}_{\mathcal{M}_2}(S \# D^{\#n-p-1})$. The first fact follows because the homeomorphism type of the surface $(S \# D^{\#n}) \setminus \sigma$ obtained by cutting along a non-separating system of arcs $\sigma = \langle [a_0], \dots, [a_p] \rangle \in \mathcal{B}^\nu(S \# D^{\#n}, b_0, b_1)$ is completely determined by the ordering of the arcs at the endpoints b_0 and b_1 , and any homeomorphism $f: (S \# D^{\#n}) \setminus \sigma \cong (S \# D^{\#n}) \setminus \sigma'$ extends to a self-homeomorphism of S which takes σ to σ' (see [14, Lem 3.2]). The second fact uses that the cut surface $S \setminus \sigma$ along a disordered system of arcs σ is canonically identified with the underlying surface of $S \# D^{\#n-p-1}$ for any p -simplex in the disordered arc complex. Indeed, this homeomorphism type does not depend on the simplex by transitivity of the action, so it is enough to check the claim for any chosen simplex. Let

$$\sigma_p = \langle \rho_{n-p}, \dots, \rho_n \rangle$$

be the collection of arcs in $S \# D^{\#n}$ consisting of the cores ρ_i of the last $p+1$ disks. Recall from Lemma 4.2 that this is a disordered simplex, once we note additionally that the arcs are also non-separating. Now Figure 9 shows that the operation of cutting along the core ρ of a disk exactly undoes the gluing operation, which proves the claim in that case.

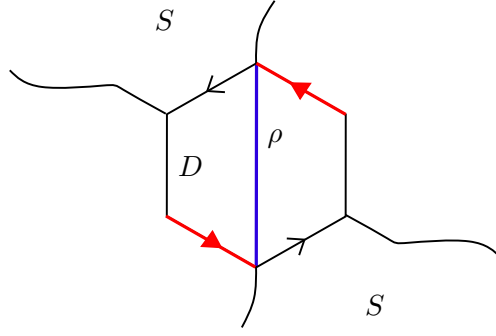


Figure 9: Cutting along the core of a disk

Note that the actions on both sets of simplices are given by post-composition with mapping classes, where we think here of an arc as an isotopy class of embedding. There is then a unique equivariant isomorphism $\varphi_p: W_n(S, D)_p \xrightarrow{\cong} \mathcal{D}^\nu(S \# D^{\#n})_p$ taking the p -simplex

$$f_p = (S \# D^{\#n-p-1}, \text{id}_{S \# D^{\#n}})$$

of $W_n(S, D)$ to the p -simplex $\sigma_p = \langle \rho_{n-p}, \dots, \rho_n \rangle$ of the target already considered above.

We are left to check that the face maps d_i correspond to each other under the isomorphisms φ_p . Because the face maps are equivariant with respect to the $\text{Aut}_{\mathcal{M}_2}(S \# D^{\#n})$ -action in both cases, and the actions are transitive, it is enough to check that the face maps agree for the simplices f_p and $\sigma_p = \varphi_p(f_p)$. By definition,

$$d_i f_p = ((S \# D^{\#n-p-1}) \# D, \text{id}_{S \# D^{\#n-p-1}} \# b_{D^{\#i}, D}^{-1} \# \text{id}_{D^{\#p-i}})$$

while

$$d_i \sigma_p = \langle \rho_{n-p}, \dots, \widehat{\rho_{n-p+i}}, \dots, \rho_n \rangle$$

is the simplex obtained by forgetting the $(i+1)$ st arc. In particular, we immediately have that $d_0(f_p) = f_{p-1}$ and $d_0(\sigma_p) = \sigma_{p-1} = \varphi_{p-1}(f_{p-1})$ giving that the face maps agree in that case.

For the remaining face maps, note that

$$\text{id}_{S \# D^{\#n-p-1}} \# b_{D^{\#i}, D}^{-1} \oplus \text{id}_{D^{\#p-i}} = T_{n-p+i-1} \circ \dots \circ T_{n-p}: S \# D^{\#n} \longrightarrow S \# D^{\#n}$$

as composition of Dehn twists T_i of Section 3.2. We need to compute the image of $\rho_{n-p+1}, \dots, \rho_n$ under this map. By Lemma 4.3, we have that for $1 \leq j \leq i$,

$$\begin{aligned} T_{n-p+i-1} \circ \dots \circ T_{n-p}(\rho_{n-p+j}) &= T_{n-p+i-1} \circ \dots \circ T_{n-p+j-1}(\rho_{n-p+j}) \\ &= T_{n-p+i-1} \circ \dots \circ T_{n-p+j}(\rho_{n-p+j-1}) \\ &= \rho_{n-p+j-1} \end{aligned}$$

while for $i+1 \leq j \leq p$,

$$T_{n-p+i-1} \circ \dots \circ T_{n-p}(\rho_{n-p+j}) = \rho_{n-p+j}.$$

Hence $d_i(f_p)$ takes the arcs $\rho_{n-p+1}, \dots, \rho_n$ to the arcs

$$\rho_{n-p}, \dots, \rho_{n-p+i-1}, \rho_{n-p+i+1}, \dots, \rho_n,$$

i.e. precisely to the arcs of $d_i(\sigma_p)$. So we indeed have that $\varphi_{p-1}(d_i(f_p)) = d_i(\varphi_{p-1}(f_p))$, which finishes the proof. \square

4.2 Coefficient systems Having identified the space of destabilizations with the semi-simplicial set of disordered arcs in Proposition 4.4, we can now input the connectivity computation of the disordered arc complex of Section 2 into the general stability theorem of [22]. To state the resulting stability theorem in full generality, we need to introduce the notions of (split) finite degree coefficient systems. We follow [22, Sec 4], which generalizes [25, 4.1-4] that unify the earlier definitions of Dwyer for the general linear groups [8] and Ivanov for the mapping class groups [19]. (The papers [22, 25] consider in addition abelian coefficient systems, but these are not relevant here, because the abelianization of the mapping class group of surfaces of large enough genus is trivial by a theorem of Mumford–Birman–Powell, see Lemma 1.1 in [13].)

Fix a bidecorated surface $S = (S, m, \varphi)$, and let D be the bidecorated disk as above. Definition 4.1 of [22] becomes in our case:

Definition 4.5. A *coefficient system* for the groups $\text{Aut}_{\mathcal{M}_2}(S \# D^{\#n})$ with respect to the stabilization by D is a collection of $\mathbb{Z}[\text{Aut}(S \# D^{\#n})]$ -modules M_n for $n \geq 0$, together with maps $s_n: M_n \rightarrow M_{n+1}$ which are equivariant with respect to the stabilization map $\text{Aut}(S \# D^{\#n}) \xrightarrow{\#D} \text{Aut}(S \# D^{\#n+1})$, satisfying the following condition:

$$(4.1) \quad T_{n+1} \in \text{Aut}(S \# D^{\#n+2}) \text{ acts trivially on the image of } M_n \xrightarrow{s_{n+1} \circ s_n} M_{n+2}$$

for T_{n+1} the Dehn twist of Section 3.2 with support the last two disks in $S \# D^{\#n+2}$.

We will encode the data of a coefficient system as a pair (F, σ^F) with

$$F: \mathcal{M}_2|_{S,D} \rightarrow \text{Mod}_{\mathbb{Z}}$$

a functor from the full subcategory of \mathcal{M}_2 on the objects $S \# D^{\#n}$ for $n \geq 0$ to abelian groups, where $M_n = F(S \# D^{\#n})$ with its $\text{Aut}(S \# D^{\#n})$ -action induced by F , and

$$\sigma^F: F(-) \rightarrow F(- \# D)$$

is a natural transformation encoding the suspension maps s_n , where we assume that $F(\text{id} \# T)$ acts trivially on the image of $(\sigma^F)^2: F(-) \rightarrow F(- \# D^{\#2})$ for T the Dehn twist supported on the added disks $D^{\#2}$.

Given a coefficient system F , define its *suspension* $\Sigma F: \mathcal{M}_2|_{S,D} \rightarrow \text{Mod}_{\mathbb{Z}}$ to be given by $\Sigma F(-) = F(- \# D)$ where

$$\sigma^{\Sigma F}: \Sigma F(-) = F(- \# D) \xrightarrow{\sigma^F} F(- \# D^{\#2}) \xrightarrow{\text{id} \# T} F(- \# D^{\#2}) = \Sigma F(- \# D),$$

where one checks that the triviality condition (4.1) is satisfied with this choice of structure map $\sigma^{\Sigma F}$. (See [22, Def 4.4].)

The structure map σ^F induces a natural transformation $F \rightarrow \Sigma F$, called the *suspension map*. We define the *kernel* $\ker F$ and *cokernel* $\text{coker} F$ to be the kernel and cokernel functors of that natural transformation. We call F *split* if the suspension map is split injective in the category of coefficient systems.

Definition 4.6. [25, Def 4.10] A coefficient system F is

- (a) of *(split) degree* -1 at N if $F(S \# (D^{\#n})) = 0$ for all $n \geq N$;
- (b) of *degree* $k \geq 0$ at N if $\ker(F)$ has degree -1 at N and $\text{coker}(F)$ has degree $(k - 1)$ at $(N - 1)$;

- (c) of *split degree* $k \geq 0$ at N if F is split and $\text{coker}(F)$ is of split degree $(k - 1)$ at $(N - 1)$.

Example 4.7.

- (a) A coefficient system F is of degree 0 at 0 if and only if σ^F is a natural isomorphism. This is in particular the case for constant coefficient systems.
- (b) The functor $F_k: \mathcal{M}_2 \rightarrow \text{Mod}_{\mathbb{Z}}$ defined by

$$F_k(S) = H_1(S, \mathbb{Z})^{\otimes k}$$

is a split coefficient system of degree k at 0. (This is essentially a result of Ivanov [19, Sec 2.8], who considers a version of the composite stabilization $\#D^{\#2}$. See also [6, Ex 4.3] for the case $k = 1$, and [26, Lem 2.9] which proves this in a very general set-up, though in the case of a braided groupoid acting over itself only.)

- (c) Given a k -connected space X , the coefficient system $F_n^k: \mathcal{M}_2 \rightarrow \text{Mod}_{\mathbb{Z}}$ defined by

$$F_n^k(S) = H_n(\text{Map}(S/\partial S), X),$$

which appears in the work of Cohen–Madsen [7], is a coefficient system of degree $\lfloor n/k \rfloor$ (see [6, Ex 4.3]).

Remark 4.8. Although the above examples all makes sense in the different set-ups considered in the literature, one should keep in mind that there are variations in what precisely a finite degree coefficient system for the mapping class groups of surfaces means in e.g. the papers [19, 7, 6, 25] and [22]. This is due to two facts: first, the definition of the coefficient system depends on the category of surfaces considered and on the stabilization $\text{map}(s)$ one works with, and second, the triviality condition (4.1) arising from Krannich’s framework is actually weaker than the one used in earlier frameworks, see e.g. [22, Rem 7.9].

In addition, the paper [11] uses a homological condition instead of a finite degree condition (see 5.5.1 in that paper). The relationship between that condition and finite degree conditions is discussed in [10, Rem 19.11].

4.3 The stability theorem We are now ready to state our main theorem:

Theorem 4.9. *Let $S = (S, m, \varphi)$ be an object of \mathcal{M}_2 with m odd, i.e. such that I_0, I_1 are in the same boundary component. Let $F: \mathcal{M}_2|_{S,D} \rightarrow \text{Mod}_{\mathbb{Z}}$ be a coefficient system and write $F_n = F(S \# D^{\#n})$. The map*

$$H_i(\text{Aut}_{\mathcal{M}_2}(S \# D^{\#n}); F_n) \rightarrow H_i(\text{Aut}_{\mathcal{M}_2}(S \# D^{\#n+1}); F_{n+1})$$

is

- (a) an epimorphism for $i \leq \frac{n}{3}$ and an isomorphism for $i \leq \frac{n-3}{3}$ if F is constant.
- (b) an epimorphism for $i \leq \frac{n-3k-2}{3}$ and an isomorphism for $i \leq \frac{n-3k-5}{3}$ if F has degree k at $N \geq 0$ and $n > N$.
- (c) an epimorphism for $i \leq \frac{n-k-2}{3}$ and an isomorphism for $i \leq \frac{n-k-5}{3}$ if F has split degree k at $N \geq 0$ and $n > N$.

Remark 4.10. We have stated the theorem in the case of an initial surface S with I_0 and I_1 in the same boundary component for simplicity. The case of a surface S' where the two intervals lie in different components is actually also included in the statement, by writing $S' = S \# D$ for S of the previous type, or considering $S' \# D$ if S' does not admit such a decomposition. Indeed, as we have already seen in Section 3 (see Figure 4), gluing in a disk exactly changes whether I_0 and I_1 are in the same boundary or not.

We will first show that the above results implies the two main theorems stated in the introduction.

Proof of Theorems A and B from Theorem 4.9. Let $S_{0,r}^s$ be a surface of genus 0 with $r \geq 1$ boundary components and s punctures, and consider the associated object $S = (S_{0,r}^s, 1, \varphi)$ of \mathcal{M}_2 , with two marked intervals in the first boundary component. Then $S \# D^{\#2g}$ has the form $(S_{g,r}^s, 1 + 2g, \varphi)$ while $S \# D^{\#2g+1}$ has the form $(S_{g,r+1}^s, 2 + 2g, \varphi)$. Moreover, the maps

$$S \# D^{\#2g} \xrightarrow{\#D} S \# D^{\#2g+1} \xrightarrow{\#D} S \# D^{\#2g+2}$$

precisely induce on automorphism groups in \mathcal{M}_2 the two maps appearing in Theorems A and B.

The fact that the first map is always injective in homology follows from the fact that postcomposing the map $S_{g,r}^s \rightarrow S_{g,r+1}^s$, defined by the sum $\#D$, with the map $S_{g,r+1}^s \rightarrow S_{g,r+1}^s \cup_{S^1} D^2 \simeq S_{g,r}^s$ filling in one of the newly created boundary component, is homotopic to the identity. Now Theorem 4.9(a) gives that the map

$$H_i(\text{Aut}_{\mathcal{M}_2}(S \# D^{\#2g})) \xrightarrow{\#D} H_i(\text{Aut}_{\mathcal{M}_2}(S \# D^{\#2g+1}))$$

is surjective for $i \leq \frac{2g}{3}$ in homology with constant coefficients. Given that the map is always injective, we get an isomorphism in that same range, proving the first part of Theorem A. Applying (b) and (c) instead gives Theorem B for the first map.

For the second map, we now apply Theorem 4.9 in the case $n = 2g + 1$, but in that case, there is no additional argument for injectivity, so the bounds translate directly to surjectivity and isomorphism bounds. \square

Proof of Theorem 4.9. Proposition 4.4 together with Theorem 2.5 give that $W_n(S, D)_\bullet$ is $\left(\frac{2g+\nu-5}{3}\right)$ -connected, for g the genus of $S \# D^{\#n}$ and $\nu = 1$ if I_0 and I_1 are in the same boundary component of $S \# D^{\#n}$, which is the case precisely when n is even, and $\nu = 2$ otherwise. The surface $S \# D^{\#n}$ has genus greater than or equal to the genus of $D \# D^{\#n}$, which is $\frac{n}{2}$ if n is even and $\frac{n-1}{2}$ if n is odd (see Lemma 3.1). Hence $2g + \nu \geq n + 1$ in both cases, and $W_n(S, D)_\bullet$ is at least $\left(\frac{n-4}{3}\right)$ -connected.

Now $W_n(S, D)_\bullet$ is the semi-simplicial set denoted $W^{\text{RW}}(S \# D^{\#n})_\bullet$ in [22] (see Definition 7.5 in that paper). By Lemma 7.6 in the same paper, using Proposition 3.4, this semi-simplicial set has the same connectivity as the semi-simplicial space $W(S \# D^{\#n})_\bullet$ of [22], which by Remark 2.7 of that paper determines the connectivity assumption of Theorem A in that paper: the canonical resolution of the assumption of the theorem is m -connected, if and only if the space $W(S \# D^{\#n})_\bullet$ is $(m - 1)$ -connected. Given that $W(S \# D^{\#n})_\bullet$ is $\left(\frac{n-4}{3}\right)$ -connected, we have that the canonical resolution of is $\left(\frac{n-4+3}{3}\right)$ -connected. Hence we can apply [22, Thm A] with $k = 3$ and grading $g_{\mathcal{M}_2} : \mathcal{M}_2|_{S,D} \rightarrow \mathbb{N}$ given by $g_{\mathcal{M}_2}(S \# D^{\#n}) = n - 2$; see also [22, Rem 2.24], where we can take $m = 4$. The theorem, with the improvement given by (i) in the remark, then gives that

$$H_i(\text{Aut}_{\mathcal{M}_2}(S \# D^{\#n}); \mathbb{Z}) \rightarrow H_i(\text{Aut}_{\mathcal{M}_2}(S \# D^{\#n+1}); \mathbb{Z})$$

is an isomorphism for $i \leq \frac{n-3}{3}$ and an epimorphism for $i \leq \frac{n}{3}$, giving the stated result in the case of constant coefficients. For a coefficient system F of degree k at N , [22, Thm C] gives that

$$H_i(\text{Aut}_{\mathcal{M}_2}(S \# D^{\#n}); F_n) \rightarrow H_i(\text{Aut}_{\mathcal{M}_2}(S \# D^{\#n+1}); F_{n+1})$$

is an isomorphism for $i \leq \frac{n-3k-5}{3}$ and an epimorphism for $i \leq \frac{n-3k-2}{3}$ for $n > N$, improved to an isomorphism for $i \leq \frac{n-k-5}{3}$ and an epimorphism for $i \leq \frac{n-k-2}{3}$ if F is split. \square

Remark 4.11 (Optimality of the stability bounds). Combining the two maps in Theorem A, we obtain that the genus stabilization

$$H_i(\Gamma(S_{g,r}^s); \mathbb{Z}) \longrightarrow H_i(\Gamma(S_{g+1,r}^s); \mathbb{Z})$$

is an epimorphism when $i \leq \frac{2g}{3}$ and an isomorphism when $i \leq \frac{2g-2}{3}$. The slope $\frac{2}{3}$ is known to be optimal by a computation of Morita [23], with optimal isomorphism range since for instance $H_1(\Gamma(S_{2,r}); \mathbb{Z}) \longrightarrow H_1(\Gamma(S_{3,r}); \mathbb{Z})$ is not injective as the source is isomorphic to $\mathbb{Z}/12$ and the target is trivial, see e.g. [21, Theorem 5.1]. Our combined genus epimorphism range, on the other hand, falls short of the range $i \leq \frac{2g+1}{3}$, as given in [11], a range that is optimal by Morita’s computation (see Theorem B (i) of [11]).

Our results for twisted coefficients are most easily compared with those of Boldsen [6, Thm 3], whose coefficient systems are coefficient systems of finite split degree in our sense, though with a stricter triviality condition upon double stabilization. For these coefficient systems, he obtains slightly better ranges, with improvement $+\frac{2}{3}$ for the first map and $+\frac{5}{3}$ for the second. The papers [25, 11] only consider genus stability. In [25], the stability slope obtained is only $\frac{1}{2}$, while in [11, Sec 5.5.1], the finite degree condition is replaced by a more general homological condition that applies to some finite coefficient systems [10, Sec 19.2]. In the particular case of the k th tensor power of the first homology of the surface, they do however only get the epimorphism range $i \leq \frac{2g-2k+1}{3}$ and isomorphism range $i \leq \frac{2g-2k-2}{3}$, see Example 5.22 in that paper.

5. Braiding and homological stability for groups

In order to use the framework of Krannich [22] to prove homological stability for a sequence of groups, one needs the structure of an “ E_1 -module over an E_2 -algebra”. We give in Proposition 5.1 below a simple way to construct such a module structure, in terms of Yang–Baxter operators. Compared to earlier approaches to homological stability such as [25], which Krannich’s work generalizes, this has the advantage of being very lightweight. Instead of having to provide the structure of a braiding on the monoidal category whose automorphism groups one is interested in, it suffices to provide a single morphism satisfying a simple equation.

Our main example of a Yang–Baxter operator is the inverse Dehn twist $T_1^{-1} \in \text{Aut}_{\mathcal{M}_2}(D \# D)$, defined in Section 3.2 and used to prove our main result. In Section 5.3, we show that this Yang–Baxter operator is not part of a braided monoidal structure on the category \mathcal{M}_2 , but gives instead a twisted version of such a structure.

5.1 Yang–Baxter operators and braid groupoid actions Let $\mathcal{X} = (\mathcal{X}, \oplus, \mathbb{1})$ be a monoidal category. A *Yang–Baxter operator* in \mathcal{X} is a pair (X, τ) consisting of an object $X \in \mathcal{X}$ and a morphism $\tau \in \text{Aut}_{\mathcal{X}}(X \oplus X)$, satisfying the Yang–Baxter equation

$$(\tau \oplus 1)(1 \oplus \tau)(\tau \oplus 1) = (1 \oplus \tau)(\tau \oplus 1)(1 \oplus \tau) \in \text{Aut}_{\mathcal{X}}(X \oplus X \oplus X),$$

where we suppress associators from the notation.

Yang–Baxter operators are closely related to the braid groupoid: Recall from Section 3.2 the braid groupoid \mathcal{B} , with objects the natural numbers and only non-trivial morphisms $\text{Aut}_{\mathcal{B}}(n) = B_n$. A variant of the coherence theorem for braided monoidal categories says that the category of strong monoidal functors from the braid groupoid into \mathcal{X} is equivalent to a naturally defined

category of Yang–Baxter operators in \mathcal{X} [20, Prop 2.2].⁴ To a Yang–Baxter operator (X, τ) in \mathcal{X} , this equivalence associates the strong monoidal functor $\Phi_{X,\tau}: \mathcal{B} \rightarrow \mathcal{X}$ given by $\Phi_{X,\tau}(n) = X^{\oplus n}$ on objects, and on morphisms by letting

$$\Phi_{X,\tau}: B_n \longrightarrow \text{Aut}_{\mathcal{X}}(X^{\oplus n})$$

send the i th standard generator σ_i to $\text{id}_{X^{\oplus i-1}} \oplus \tau \oplus \text{id}_{X^{\oplus n-i-1}}$, where the required maps $\Phi_{X,\tau}(m) \oplus \Phi_{X,\tau}(n) \rightarrow \Phi_{X,\tau}(m+n)$ are given by the monoidal structure of \mathcal{X} .

Suppose now that the monoidal category \mathcal{X} acts on a category \mathcal{M} via a functor $\mathcal{M} \times \mathcal{X} \rightarrow \mathcal{M}$, which we also denote by \oplus , compatible with the monoidal sum in \mathcal{X} . The following result shows that the choice of a Yang–Baxter operator defines an action of the braid groupoid \mathcal{B} on \mathcal{M} , and hence is appropriate data to apply the stability framework of [22]:

Proposition 5.1. *Let $(\mathcal{X}, \oplus, \mathbb{1})$ be a monoidal category with $\tau \in \text{Aut}_{\mathcal{X}}(X \oplus X)$ a Yang–Baxter operator in \mathcal{X} . Suppose \mathcal{X} acts on a category \mathcal{M} . Then there is an action of the braid groupoid*

$$\alpha_\tau: \mathcal{M} \times \mathcal{B} \longrightarrow \mathcal{M}$$

given on objects by $\alpha_\tau(A, n) = A \oplus X^{\oplus n}$ and determined on morphisms by

$$\alpha_\tau(f, \sigma_i) = f \oplus \text{id}_{X^{\oplus i-1}} \oplus \tau \oplus \text{id}_{X^{\oplus n-i-1}},$$

for σ_i the i th elementary braid in B_n . Furthermore, taking classifying spaces this endows $B\mathcal{M}$ with the structure of an E_1 -module over the E_2 -algebra $B\mathcal{B}$.

Note that if we are interested in homological stability for stabilization by X for the automorphism groups $G_n := \text{Aut}_{\mathcal{M}}(A \oplus X^{\oplus n})$ for some object A of \mathcal{M} , only the full subcategory $\mathcal{M}_{A,X} \subseteq \mathcal{M}$ spanned by objects of the form $A \oplus X^{\oplus n}$, is relevant. So for stability purposes, it is enough to consider the subfunctor

$$\alpha_\tau: \mathcal{M}_{A,X} \times \mathcal{B} \longrightarrow \mathcal{M}_{A,X}.$$

In fact, to make sure that the structure of E_1 -module over the E_2 -algebra $B\mathcal{B}$ is graded, one can even replace the category $\mathcal{M}_{A,X}$ by a category with objects the natural numbers and setting $\text{Aut}(n) = \text{Aut}_{\mathcal{M}}(A \oplus X^{\oplus n})$, avoiding any potential issue coming from unwanted equalities $A \oplus X^{\oplus n} = A \oplus X^{\oplus m}$ for $m \neq n$.

Proof. The functor $\alpha_\tau: \mathcal{M} \times \mathcal{B} \rightarrow \mathcal{M}$ is defined as the composite functor

$$\alpha(-, -) = (-) \oplus \Phi_{X,\tau}(-),$$

for $\Phi_{X,\tau}: \mathcal{B} \rightarrow \mathcal{X}$ as above. The result follows from [22, Lem 7.2] because α makes \mathcal{M} into a module over \mathcal{B} and \mathcal{B} is braided monoidal. \square

Example 5.2. If $\mathcal{X} = (\mathcal{X}, \oplus, \mathbb{1})$ admits a braiding b , then $\tau = b_{X,X} \in \text{Aut}_{\mathcal{X}}(X \oplus X)$ is a Yang–Baxter operator for any object X . For \mathcal{X} a groupoid acting on itself or \mathcal{X} acting on a category \mathcal{M} , this recovers the basic set-up for homological stability of the paper [25], or Section 7 of [22].

⁴In other words, the pair consisting of the braid groupoid \mathcal{B} and the Yang–Baxter operator $\sigma_1 \in \text{Aut}_{\mathcal{B}}(2)$, is the initial monoidal category with a distinguished Yang–Baxter element.

Example 5.3 (Mapping class groups of surfaces). As explained above, a Yang–Baxter operator $\tau \in \text{Aut}_{\mathcal{X}}(X \oplus X)$ gives in particular a collection of homomorphisms $\Phi_{X,\tau}: B_n \longrightarrow \text{Aut}_{\mathcal{X}}(X^{\oplus n})$ from the braid groups to the automorphism group of n copies of X . There are two standard ways to embed braid groups in mapping class groups of surfaces, and we explain here how they both come from Yang–Baxter elements in appropriate categories of surfaces.

- (a) Let \mathcal{M}_2 be the category of bidecorated surfaces of Section 3. As explained in Section 3.2, the Dehn twist $T \in \text{Aut}_{\mathcal{M}_2}(D \# D) \cong \pi_0 \text{Homeo}_{\partial}(S^1 \times I) \cong \mathbb{Z}$, or its inverse T^{-1} , is a Yang–Baxter operator. The associated map $\Phi_{D,T}: B_n \longrightarrow \text{Aut}_{\mathcal{M}_2}(D^{\#n})$ is the embedding of braid group in the mapping class groups of $S_{g,1}$ (when $n = 2g + 1$) and of $S_{g,2}$ (when $n = 2g + 2$) associated to Dehn twists along the chain of embedded curves in the surfaces described in Lemma 3.5. This embedding goes back at least to the work of Birman and Hilden [3, 4].
- (b) Let \mathcal{M}_1 denote instead the category of surfaces decorated by a single interval, with monoidal structure \oplus defined just as in the case of \mathcal{M}_1 but gluing only along one interval. Then \mathcal{M}_1 is braided monoidal, see [25, Sec 5.6.1]. Hence by Example 5.2, for any object X of \mathcal{M}_1 , we have a Yang–Baxter element $\tau_X \in \text{Aut}_{\mathcal{M}_1}(X \oplus X)$. For $X = S_{1,2}$, this can be used to prove genus stabilization (albeit with the suboptimal slope $\frac{1}{2}$), and in the case $X = S^1 \times I$ marked by an interval in one of its boundary components, we have that $X^{\oplus n}$ has underlying surface an n -legged pair of pants $D^2 \setminus (\sqcup_n \mathring{D}^2)$ and the associated morphism

$$\Phi_{X,\tau_X}: B_n \longrightarrow \text{Aut}_{\mathcal{M}_1}(X^{\oplus n}) = \pi_0 \text{Homeo}_{\partial}(D^2 \setminus (\sqcup_n \mathring{D}^2))$$

is the standard embedding of the braid group as the subgroup of the mapping class group of the multi-legged pants that does not twist the legs, see e.g. [25, Sec 5.6.1].

We will show in Proposition 5.7 below that the Yang–Baxter operator T of the first example, in the category \mathcal{M}_2 , does not come from a braiding in \mathcal{M}_2 .

5.2 Homological stability from Yang–Baxter elements Suppose we are given the data of a monoidal category $(\mathcal{X}, \oplus, \mathbb{1})$ acting on a category \mathcal{M} , along with a choice of stabilizing object $X \in \mathcal{X}$ and Yang–Baxter operator $\tau \in \text{Aut}_{\mathcal{X}}(X \oplus X)$. Proposition 5.1 above allows to apply [22, Thm A], which in this case says that for any $A \in \mathcal{M}$, there is a sequence of simplicial spaces $W_n(X, A)_{\bullet}$, for $n \geq 0$, so that if $W_n(X, A)$ is highly-connected for large n , then the sequence

$$\text{Aut}_{\mathcal{M}}(A) \xrightarrow{-\oplus X} \text{Aut}_{\mathcal{M}}(A \oplus X) \xrightarrow{-\oplus X} \text{Aut}_{\mathcal{M}}(A \oplus X \oplus X) \xrightarrow{-\oplus X} \dots$$

satisfies homological stability. Theorem B of the same paper gives in addition a stability statement with twisted coefficients. Under an injectivity assumption of the form of Proposition 3.4, this simplicial space is homotopy discrete, and modeled by the space of destabilizations as described in Definition 4.1.

Remark 5.4. The fact that (X, τ) is a Yang–Baxter operator is precisely what is needed for the collection of sets $W_n(A, X)_p$ and maps $d_i: W_n(A, X)_p \longrightarrow W_n(A, X)_{p-1}$, defined as in Definition 4.1, to assemble into a semi-simplicial set; indeed, the Yang–Baxter equation implies the necessary simplicial identities.

For a fixed monoidal category $\mathcal{X} = (\mathcal{X}, \oplus, \mathbb{1})$ acting on a category \mathcal{M} , and a stabilizing object $X \in \mathcal{X}$, the choice of Yang–Baxter element will not affect the stabilizing map, but it will affect the spaces $W_n(X, A)_{\bullet}$. The identity map $1 \in \text{Aut}_{\mathcal{X}}(X \oplus X)$ is a trivial choice of

Yang–Baxter operator. But, as is to be expected, this trivial twist is not useful for proving stability:

Proposition 5.5. *Let $\mathcal{X}, \mathcal{M}, A$ and X be as above. If we choose the Yang–Baxter operator $\tau \in \text{Aut}_{\mathcal{X}}(X \oplus X)$ to be the identity element, then the semi-simplicial set $W_n(A, X)_\bullet$ is connected if and only if the map*

$$G_{n-1} = \text{Aut}_{\mathcal{M}}(A \oplus X^{\oplus n-1}) \xrightarrow{-\oplus X} \text{Aut}_{\mathcal{M}}(A \oplus X^{\oplus n}) = G_n$$

is an isomorphism.

Proof. If τ is the identity element, all face maps d_i are equal to the canonical map $G_n/G_{n-p-1} \rightarrow G_n/G_{n-p}$. In particular, the vertices of any p -simplex are all equal, so the semi-simplicial set $W_n(A, X)_\bullet$ is isomorphic to a disjoint union of semi-simplicial sets, one for each 0-simplex. The result follows from the fact that the set of 0-simplices is precisely the quotient G_n/G_{n-1} . \square

In fact, Barucco proved in his master thesis a result that translates to the following stronger statement (stated in the thesis in the context of a groupoid acting on itself, i.e. $\mathcal{M} = \mathcal{X}$):

Lemma 5.6. [2, Lem 3.1] *The space $W_n(A, X)$ is connected if and only if $1^{\oplus n-2} \oplus \tau$ and $G_{n-1} \oplus 1$ together generate $G_n = \text{Aut}(A \oplus X^{\oplus n})$.*

The connectivity of the semi-simplicial set $W_n(A, X)$ (or of the associated simplicial complex defined in [25, Def 2.8]) may be seen as a measure of the *higher generation* of the group G_n by the cosets of the subgroups G_{n-p} for $p \geq 1$ and braid subgroups generated by the chosen Yang–Baxter element t , in a way that is similar to the notion of higher generation for a family of subgroups of a group as defined in [1, 2.1].

5.3 Braidings and bidecorated surfaces We show in this section that the Yang–Baxter operator T on the bidecorated disk D in the groupoid \mathcal{M}_2 does not come from a braiding on the subcategory of \mathcal{M}_2 generated by the disk. In fact, we will show that this subcategory does not admit a braiding.

Let $D = (D^2, 1, \text{id})$ be the standard bidecorated disk of Section 3, where we recall that $X_1 = D^2$. We define a “rotated” bidecorated disk $\bar{D} = (D^2, 1, r_\pi)$, where r_π is the rotation of $\partial X_1 = \partial D^2$ by π radians, which has the effect of interchanging the intervals I_0 and I_1 . Rotating all of D^2 by π then induces a morphism $\iota: D \rightarrow \bar{D}$ in \mathcal{M}_2 , and likewise morphisms

$$\iota^{\#m}: D^{\#m} \rightarrow \bar{D}^{\#m}$$

for every $m \geq 1$, each which we will by abuse of notation also denote by ι . The morphism ι can be identified with the hyperelliptic involution of the underlying surface depicted in Figure 10 for the two cases $m = 2g$ and $m = 2g + 1$, where in the latter case the boundary components are exchanged by ι . The morphism ι induces an identification

$$\begin{aligned} \text{Aut}_{\mathcal{M}_2}(D^{\#m}) &\xrightarrow{\cong} \text{Aut}_{\mathcal{M}_2}(\bar{D}^{\#m}) \\ f &\longmapsto \iota \circ f \circ \iota^{-1} \end{aligned}$$

In order to precisely state the failure of T to extend to a braiding, we will also need the identification

$$\begin{aligned} I: \text{Aut}_{\mathcal{M}_2}(D^{\#m}) &\xrightarrow{\cong} \text{Aut}_{\mathcal{M}_2}(\bar{D}^{\#m}) \\ f &\longmapsto f \end{aligned}$$

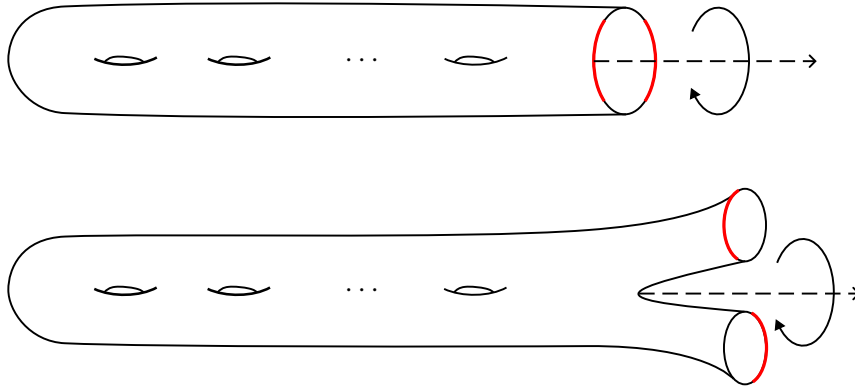


Figure 10: The hyperelliptic involutions ι of $S_{g,1}$ and $S_{g,2}$

that comes from the fact that an element $f \in \text{Aut}_{\mathcal{M}_2}(D^{\#m})$ is just a mapping class for the underlying surface of $D^{\#m}$, which is the same as the underlying surface of $\bar{D}^{\#m}$, so f can just as well be viewed as an element of $\text{Aut}_{\mathcal{M}_2}(\bar{D}^{\#m})$. In contrast with the identification induced by ι , the second identification is “external”, in the sense that it does not come from a morphism in \mathcal{M}_2 .

Viewing ι as a diffeomorphism of the underlying surface X_m of $D^{\#m}$ which does not fix the boundary, and specifically exchanges the marked points $b_0 = I_0(1/2)$ and $b_1 = I_1(1/2)$, we see that it takes the isotopy class of arc ρ_i of Section 4.1 to the reversed arc ρ_i^{-1} . We will use in the proof of the following result that the homotopy classes ρ_i generate the fundamental groupoid of X_m based at the points b_0, b_1 .⁵ The mapping class ι is in fact completely determined by the fact that $\iota(\rho_i) = \rho_i^{-1}$.

Proposition 5.7. *Let $\mathcal{D} \subset \mathcal{M}_2$ denote the full monoidal subcategory generated by D .*

(i) *The monoidal category \mathcal{D} does not admit a braiding. In particular, the monoidal functor*

$$\Phi: (\mathcal{B}, \oplus) \longrightarrow (\mathcal{D}, \#) \subset (\mathcal{M}_2, \#)$$

does not come from a braiding on \mathcal{D} .

(ii) *Let $f \in \text{Aut}_{\mathcal{M}_2}(D^{\#m})$ and $g \in \text{Aut}_{\mathcal{M}_2}(D^{\#n})$, and put $\beta_{m,n} = \Phi(b_{m,n})$, where the block braid $b_{m,n}$ is the braid which passes the last n strands over the first m strands. Then*

$$\beta_{m,n} \circ (f \# g) \circ \beta_{n,m}^{-1} = \begin{cases} g \# (\iota^{-1} \circ f \circ \iota) & \text{if } n \text{ is odd,} \\ g \# f & \text{else,} \end{cases}$$

for $\iota: D^{\#m} \longrightarrow \bar{D}^{\#m}$ the involution defined above, and where f in the rightmost expression is the map f considered as an element of $\text{Aut}_{\mathcal{M}_2}(\bar{D}^{\#m})$ via the isomorphism I defined above.

Proof. We start by proving (ii). It is enough to check the statement when f and g are Dehn twists, as those generate the mapping class groups. Note that if c is a curve in the underlying surface X_{m+n} of $D^{\#m+n}$, and T_c denotes the Dehn twist along c , then conjugating T_c by a diffeomorphism φ of the surface gives

$$\varphi \circ T_c \circ \varphi^{-1} = T_{\varphi(c)}.$$

⁵As a full subgroupoid of the ordinary fundamental groupoid of X_m , this groupoid is the one spanned by the objects corresponding to the points $b_0, b_1 \in X_m$.

Recall further that the isotopy class of a Dehn twist T_c depends only on the free homotopy class of the curve c . We are therefore to compute the images of curves in $D^{\#m}$ and $D^{\#n}$ under the map $\beta_{m,n}$, as free homotopy classes. A curve c can be written, up to free homotopy, as a concatenation of the arcs ρ_i and their inverses ρ_i^{-1} , as the homotopy classes of these arcs generate the fundamental groupoid of the surface X_{m+n} based at b_0, b_1 . In particular, write

$$(5.1) \quad c \simeq \rho_{i_1} * \rho_{i_2}^{-1} * \rho_{i_3} \cdots * \rho_{i_k}^{-1}.$$

The mapping class $\beta_{m,n}$ can be written as the composition

$$\beta_{m,n} = (T_n \circ \cdots \circ T_{m+n-1}) \circ \cdots \circ (T_2 \circ \cdots \circ T_{m+1}) \circ (T_1 \circ \cdots \circ T_m)$$

and hence we can compute the image of each ρ_i using Lemma 4.3. For $r > 0$, denote by $T_{i,i+r}$ the composition of Dehn twists $T_i \circ T_{i+1} \circ \cdots \circ T_{i+r}$. Note first that

$$T_{i,j}(\rho_{j+1}) \simeq T_{i,j-1}(\rho_j) \simeq \cdots \simeq \rho_i.$$

From this, it follows that for $i \geq 1$,

$$\begin{aligned} \beta_{m,n}(\rho_{m+i}) &\simeq (T_{n,m+n-1}) \circ \cdots \circ (T_{1,m})(\rho_{m+i}) \\ &\simeq (T_{n,m+n-1}) \circ \cdots \circ (T_{i,m+i-1})(\rho_{m+i}) \\ &\simeq (T_{n,m+n-1}) \circ \cdots \circ (T_{i+1,m+i})(\rho_i) \\ &\simeq \rho_i. \end{aligned}$$

On the other hand, for $i \leq k \leq j$, we have

$$T_{i,j}(\rho_k) \simeq T_{i,k}(\rho_k) \simeq T_{i,k-1}(\rho_k * \rho_{k+1}^{-1} * \rho_k) \simeq \rho_i * \rho_{k+1}^{-1} * \rho_i,$$

from which we can deduce that for $i \leq m$,

$$\begin{aligned} \beta_{m,n}(\rho_i) &\simeq (T_{n,m+n-1}) \circ \cdots \circ (T_{1,m})(\rho_i) \\ &\simeq (T_{n,m+n-1}) \circ \cdots \circ (T_{2,m+1})(\rho_1 * \rho_{i+1}^{-1} * \rho_1) \\ &\simeq (T_{n,m+n-1}) \circ \cdots \circ (T_{3,m+2})(\rho_1 * \rho_2^{-1} * \rho_{i+2} * \rho_2^{-1} * \rho_1) \\ &\simeq \cdots \\ &\simeq \rho_1 * \iota(\rho_2) * \cdots * \iota^{n-1}(\rho_n) * \iota^n(\rho_{i+n}) * \iota^{n-1}(\rho_n) * \cdots * \iota(\rho_2) * \rho_1 \end{aligned}$$

since $\iota^j(\rho_i)$ is ρ_i when j is even and ρ_i^{-1} when j is odd.

If the curve c lies in the last n disks $D^{\#n}$ inside $D^{\#m+n}$, it can be written as a product (5.1) with each $i_j > m$. Then the above computation gives that

$$\beta_{m,n}(c) \simeq \rho_{i_1-m} * \rho_{i_2-m}^{-1} * \rho_{i_3-m} * \cdots * \rho_{i_k-m}^{-1},$$

that is, c is mapped to the corresponding curve in the *first* n disks $D^{\#n}$ inside $D^{\#n+m} = D^{\#m+n}$.

If the curve c instead lies in the first m disks $D^{\#m}$ inside $D^{\#m+n}$, it can be written as a product (5.1) with each $i_j \leq m$. Then the above computation gives that

$$\begin{aligned} \beta_{m,n}(c) &\simeq \rho_1 * \iota(\rho_2) * \cdots * \iota^{n-1}(\rho_n) * \iota^n(\rho_{i_1+n}) * \iota^{n+1}(\rho_{i_2+n}) * \cdots * \iota^{n+1}(\rho_{i_k+n}) \\ &\quad * \iota^n(\rho_n) * \cdots * \iota^2(\rho_2) * \iota(\rho_1) \\ &\simeq \iota^n(\rho_{i_1+n}) * \iota^{n+1}(\rho_{i_2+n}) * \iota^n(\rho_{i_3+n}) \cdots * \iota^{n+1}(\rho_{i_k+n}) \\ &\simeq \iota^n(\rho_{i_1+n} * \rho_{i_2+n}^{-1} * \rho_{i_3+n} \cdots * \rho_{i_k+n}^{-1}) \end{aligned}$$

Hence c is mapped to the curve $\iota^n(c)$ in the last m disks $D^{\#m}$ inside $D^{\#n+m} = D^{\#m+n}$, from which the statement follows.

We are left to prove (i). To see that the images $\beta_{m,n}$ of block braids under β do not define a braiding in \mathcal{D} , using (ii) it is enough to find a curve c in $D^{\#m}$ for some m so that $\iota(c) \not\cong c$, and such curves are plentiful. The same argument shows that the inverses $\beta_{m,n}^{-1}$ likewise do not define a braiding.

Now suppose that $\tilde{\beta}$ is a braiding on \mathcal{D} . The braiding is determined by $\tilde{\beta}_{1,1} \in \text{Aut}_{\mathcal{M}_2}(D^{\#2}) \cong \mathbb{Z}$, a group generated by the Dehn twist T_1 . We have excluded the possibilities $\tilde{\beta}_{1,1} = T_1^{\pm 1}$, and $\tilde{\beta}_{1,1} = \text{id}$ is similarly ruled out using now the fact that curves are not moved at all by the identity. So assume that $\tilde{\beta}_{1,1} = T_1^k$, with $|k| > 1$. Then $\tilde{\beta}_{2,1} = T_1^k T_2^k$ would have to satisfy $T_1^k T_2^k(a_1) = a_2$ in order for naturality to hold, where T_i is the Dehn twist along the curve a_i as in Section 3.2. Applying Proposition 3.2 in [9] twice, we get that the intersection number $i(a_2, T_2^k(a_1)) = i(T_1^k(T_2^k(a_1)), T_2^k(a_1)) = |k| i(a_1, T_2^k(a_1))^2 = |k|^2 i(a_1, a_2)^4 = |k|^2$. On the other hand, using Proposition 3.4 in [9] we obtain

$$|k|^2 = i(a_2, T_2^k(a_1)) = |i(T_2^k(a_1), a_2) - |k| i(a_1, a_1) i(a_1, a_2)| \leq i(a_1, a_2) = 1,$$

where we have also used that $i(a_1, a_1) = 0$. This contradicts our assumption of $\tilde{\beta}_{1,1}$. \square

Acknowledgements

The first and third authors were partially supported by the Danish National Research Foundation through the Copenhagen Centre for Geometry and Topology (DRNF151), and the third author by the European Research Council (ERC) under the European Union Horizon 2020 research and innovation programme (grant agreement No. 772960).

References

- [1] Herbert Abels and Stephan Holz. Higher generation by subgroups. *J. Algebra*, 160(2):310–341, 1993.
- [2] Matteo Barucco. Homology instability in pre-braided homogeneous categories. https://geotop.math.ku.dk/research/past_ag_theses_and_projects/ms-theses/Baruco-MS.pdf, 2017.
- [3] Joan S Birman and Hugh M Hilden. Lifting and projecting homeomorphisms. *Archiv der Mathematik*, 23(1):428–434, 1972.
- [4] Joan S Birman and Hugh M Hilden. On isotopies of homeomorphisms of Riemann surfaces. *Annals of Mathematics*, 97(3):424–439, 1973.
- [5] Søren K. Boldsen. Different versions of mapping class groups of surfaces. Preprint arXiv:0908.2221, 2009.
- [6] Søren K. Boldsen. Improved homological stability for the mapping class group with integral or twisted coefficients. *Mathematische Zeitschrift*, 270(1-2):297–329, 2012.

- [7] Ralph L. Cohen and Ib Madsen. Surfaces in a background space and the homology of mapping class groups. In *Algebraic geometry—Seattle 2005. Part 1*, volume 80 of *Proc. Sympos. Pure Math.*, pages 43–76. Amer. Math. Soc., Providence, RI, 2009.
- [8] W. G. Dwyer. Twisted homological stability for general linear groups. *Ann. of Math. (2)*, 111(2):239–251, 1980.
- [9] Benson Farb and Dan Margalit. *A Primer on Mapping Class Groups*. Princeton University Press, 2011.
- [10] Søren Galatius, Alexander Kupers, and Oscar Randal-Williams. Cellular E_k -algebras. preprint [ArXiv:1805.07184](https://arxiv.org/abs/1805.07184), 2018.
- [11] Søren Galatius, Alexander Kupers, and Oscar Randal-Williams. E_2 -cells and mapping class groups. *Publications mathématiques de l’IHÉS*, 130(1):1–61, June 2019.
- [12] André Gramain. Le type d’homotopie du groupe des difféomorphismes d’une surface compacte. *Ann. Sci. École Norm. Sup. (4)*, 6:53–66, 1973.
- [13] John L. Harer. The second homology group of the mapping class group of an orientable surface. *Inventiones Mathematicae*, 72(2):221–239, 1983.
- [14] John L. Harer. Stability of the homology of the mapping class groups of orientable surfaces. *Annals of mathematics*, 121(2):215–249, 1985.
- [15] John L. Harer. Improved stability for the homology of the mapping class groups of surfaces, 1993. Preprint.
- [16] Allen Hatcher and Karen Vogtmann. Tethers and homology stability for surfaces. *Algebr. Geom. Topol.*, 17(3):1871–1916, 2017.
- [17] Allen Hatcher and Nathalie Wahl. Stabilization for mapping class groups of 3-manifolds. *Duke Math. J.*, 155(2):205–269, 2010.
- [18] Nikolai V. Ivanov. Stabilization of the homology of Teichmüller modular groups. *Algebra i Analiz*, 1(3):110–126, 1989.
- [19] Nikolai V. Ivanov. On the homology stability for Teichmüller modular groups: closed surfaces and twisted coefficients. In *Mapping class groups and moduli spaces of Riemann surfaces (Göttingen, 1991/Seattle, WA, 1991)*, volume 150 of *Contemp. Math.*, pages 149–194. Amer. Math. Soc., Providence, RI, 1993.
- [20] André Joyal and Ross Street. Braided tensor categories. *Advances in Mathematics*, 102(1):20–78, 1993.
- [21] Mustafa Korkmaz. Low-dimensional homology groups of mapping class groups: a survey. *Turkish Journal of Mathematics*, 26(1):101–114, 2002.
- [22] Manuel Krannich. Homological stability of topological moduli spaces. *Geom. Topol.*, 23(5):2397–2474, 2019.
- [23] Shigeyuki Morita. Generators for the tautological algebra of the moduli space of curves. *Topology*, 42(4):787–819, 2003.

- [24] Oscar Randal-Williams. Resolutions of moduli spaces and homological stability. *Journal of the European Mathematical Society*, 18(1):1–81, 2016.
- [25] Oscar Randal-Williams and Nathalie Wahl. Homological stability for automorphism groups. *Advances in Mathematics*, 318:534–626, October 2017.
- [26] Arthur Soulié. Some computations of stable twisted homology for mapping class groups. *Comm. Algebra*, 48(6):2467–2491, 2020.
- [27] Nathalie Wahl. Homological stability for the mapping class groups of non-orientable surfaces. *Invent. Math.*, 171(2):389–424, 2008.
- [28] Nathalie Wahl. Homological stability for mapping class groups of surfaces. In *Handbook of Moduli: Volume III*, volume 26 of *Advanced Lectures in Mathematics*, pages 547–583. International Press of Boston, 2013.
- [29] Bronislaw Wajnryb. Artin groups and geometric monodromy. *Inventiones mathematicae*, 138(3):563–571, 1999.